Title: Does phenology explain plant-pollinator interactions at different latitudes? An assessment of its explanatory power in plant-hoverfly networks in French calcareous grasslands

Authors: Natasha de Manincor[1]*, Nina Hautekeete[1], Yves Piquot[1], Bertrand Schatz[2], Cédric Vanappelghem[3], François Massol[1,4]

[1]Université de Lille, CNRS, UMR 8198 - Evo-Eco-Paleo, F-59000 Lille, France

[2]CEFE, EPHE-PSL, CNRS, University of Montpellier, University of Paul Valéry Montpellier 3, IRD, Montpellier, France

[3]Conservatoire d'espaces naturels Nord et du Pas-de-Calais, 160 rue Achille Fanien - ZA de la Haye, 62190 LILLERS

[4]Univ. Lille, CNRS, Inserm, CHU Lille, Institut Pasteur de Lille, U1019 - UMR 8204 - CIIL - Center for Infection and Immunity of Lille, F-59000 Lille, France

E-mail addresses and ORCID numbers:

Natasha de Manincor: natasha.de-manincor@univ-lille.fr, 0000-0001-9696-125X

Nina Hautekeete: nina.hautekeete@univ-lille.fr, 0000-0002-6071-5601

Yves Piquot: yves.piquot@univ-lille.fr, 0000-0001-9977-8936

Bertrand Schatz: bertrand.schatz@cefe.cnrs.fr, 0000-0003-0135-8154

Cédric Vanappelghem: cedric.vanappelghem@espaces-naturels.fr

François Massol: francois.massol@univ-lille.fr, 0000-0002-4098-955X

Short title: Phenology and plant-hoverfly interactions

Keywords: Bayesian model, interaction probability, latent block model, latitudinal gradient, mutualistic network, phenology overlap, species abundance, structural equation model.

*Corresponding author information: Natasha de Manincor, e-mail: natasha.de-manincor@univ-lille.fr, phone: +330362268530

Author contributions

NDM and FM conceived the project, formulated and implemented the model. NDM conducted the analysis and prepared the manuscript. FM supervised the analysis and edited the manuscript. NH, YP, CV and BS contributed substantially to all later versions. NDM, NH, YP and BS conducted the fieldwork and provided the data. CV identified the hoverflies.

Data accessibility

The data supporting the results are archived on Zenodo (DOI: 10.5281/zenodo.2542845).

Abstract

For plant-pollinator interactions to occur, the flowering of plants and the flying period of pollinators (*i.e.* their phenologies) have to overlap. Yet, few models make use of this principle to predict interactions and fewer still are able to compare interaction networks of different sizes. Here, we tackled both challenges using Bayesian Structural Equation Models (SEM), incorporating the effect of phenology overlap in six plant-hoverfly networks. Insect and plant abundances were strong determinants of the number of visits, while phenology overlap alone was not sufficient, but significantly improved model fit. Phenology overlap was a stronger determinant of plant-pollinator interactions in sites where the average overlap was longer and network compartmentalization was weaker, *i.e.* at higher latitudes. Our approach highlights the advantages of using Bayesian SEMs to compare interaction networks of different sizes along environmental gradients and articulates the various steps needed to do so.

INTRODUCTION

Understanding how phenology determines species interactions is a central question in the case of mutualistic networks. In plant-pollinator networks, phenology shapes their temporal and spatial limits, thus defining the area and the period along the season in which interactions preferably occur (Olesen *et al.* 2011; Ogilvie & Forrest 2017). Since plant and pollinator phenologies are not equally affected by changes in environmental cues, partial or total phenological mismatches can occur as a result of environmental changes such as climate change (Parmesan 2007; Rafferty 2017). Phenological advances indeed increase at higher latitudes, as a response to the acceleration of warming temperature along the same gradient (Post *et al.* 2018), increase phenological mismatch, and have the potential to threaten the synchrony needed for effective pollination (Hutchings *et al.* 2018). Such environmental changes can thus drastically alter pollinator interactions through modified temporal overlap between pollinators and their floral resources leading, in extreme cases, to local extinctions (Memmott *et al.* 2007) and the ensuing absence of the partner species at the location and/or time at which the interaction should have taken place (Willmer 2012; Miller-Struttmann *et al.* 2015; Rafferty *et al.* 2015; Hutchings *et al.* 2018).

Because phenological match is crucial to plant-pollinator interactions, and thus ultimately to pollinators' fitness, pollinators have to adapt to phenological shifts either through interaction with other plant species (Rafferty *et al.* 2015) or through changes of their own phenology (Bartomeus *et al.* 2011). Phenology can then influence dynamical network properties, such as the stability and the coexistence of species, through changes in network topology (Encinas-Viso *et al.* 2012). Moreover, phenology predictably affects network compartmentalization as different phenophases likely correspond to different compartments when networks are considered on an annual scale (Martín González *et al.* 2012).

Despite considerable theoretical advances, there are few models available to predict the probability of interaction in plant-pollinator networks (Staniczenko *et al.* 2017; Cirtwill *et al.* 2019) and fewer still

able to make comparisons between networks. Due to their complexity and variation among years (Chacoff *et al.* 2017), most studies of mutualistic networks have focused on predicting and comparing classic network metrics (nestedness, connectance, modularity, etc.) which are all influenced by network size, *i.e.* the number of plant and insect species (Fortuna *et al.* 2010; Staniczenko *et al.* 2013; Poisot & Gravel 2014; Astegiano *et al.* 2015). Moreover, few studies have compared interaction networks along environmental gradients (Devoto *et al.* 2005; Schleuning *et al.* 2012; Sebastián-González *et al.* 2015; Pellissier *et al.* 2017). In order to compare networks of different sizes, a better alternative is to switch from network-derived metrics to the comparison of the probability of interaction given by regression models, which can consider multiple factors and latent variables and assume that the sampled data are just part of a larger unobserved dataset (Grace *et al.* 2010).

Calcareous grasslands are characterized by highly diverse plant communities with a high proportion of entomophilous species (Baude *et al.* 2016), thus they are a convenient model for such studies. Most plant-insect pollinator networks involve bee species (Anthophila), but recent studies have also pointed out the importance of hoverflies (Diptera: Syrphidae), which pollinate a large spectrum of wild flowering species (Klecka *et al.* 2018a) and crops (Jauker & Wolters 2008; Rader *et al.* 2011). They usually behave opportunistically, *i.e.* from being pollen generalists to specialists, only limited by morphological constraints (Iler *et al.* 2013; Klecka *et al.* 2018a; Lucas *et al.* 2018). Indeed, their generalist behaviour, at the species level, could be the result of individually specialized diets, since most pollen retrieved on hoverfly individuals usually comes from a single plant taxon (Lucas *et al.* 2018) and depends on flower availability and phenology (Cowgill *et al.* 1993; Colley & Luna 2000; Lucas *et al.* 2018). Moreover, some hoverflies have preferences regarding plant colour, morphology and inflorescence height (Branquart & Hemptinne 2000; Colley & Luna 2000; Lunau 2014; Klecka *et al.* 2018b, a).

Here we study the consequences of environmental gradients on plant-pollinator interactions, focusing on how phenology overlap affects interactions between plants and insects in six calcareous grassland

sites distributed along a latitudinal gradient. We obtained plant and insect phenologies, abundances, and interactions in all sites from April to October 2016. We modelled plant-pollinator interaction networks following a Bayesian Structural Equation Modelling approach (SEM) using latent variables, *i.e.* unobserved variables (Grace *et al.* 2010). SEM is a multivariate technique used to test several hypotheses in ecological studies. SEM analysis involves cause-effect equations to evaluate multiple causal relationship (Grace 2006; Eisenhauer *et al.* 2015) using observed and latent variables to explain some other observed variables (Grace 2006). SEM can be used to choose among competing models (Grace & Bollen 2008). Thus, SEM are well suited for studying the complexity of ecological networks. To test whether phenology affects network compartmentalization, we looked for species subgroups using a latent block model (LBM) which is among the best clustering methods for weighted networks (Leger *et al.* 2015).

The comparison of 16 SEMs and the analysis of LBMs of sampled networks evinced that phenology overlap is an important determinant of plant-pollinator interactions, but is less informative than species abundances and performs heterogeneously among sites. Our results suggest that the use of SEMs to compare networks of different sizes along an environmental gradient is an innovative approach which can help understand the structure of plant-pollinator networks.

MATERIALS AND METHODS

Study sites

We sampled plant and hoverfly species in six areas (Fig. S1) of 1 hectare each in different French regions: two sites in Hauts-de-France (Les Larris de Grouches-Luchuel, thereafter noted LAR, 50°11'22.5"N 2°22'02.9"E and Regional natural reserve Riez de Noeux les Auxi, noted R, 50°14’51.85”N 2°12’05.56”E, in départements Pas-de-Calais and Somme), two sites in Normandie (Château Gaillard – le Bois Dumont, noted CG, 49°14'7.782"N 1°24'16.445"E and les Falaises d’Orival, noted FAL, 49°04'40.08"N 1°33'07.254"E, départements: Eure and Seine Maritime) and two sites in Occitanie (Fourches, noted F, 43°56'07.00"N 3°30'46.1"E and Bois de Fontaret, noted BF, 43°55'17.71"N

3°30'06.06"E, département: Gard). The six sites are included in the European NATURA 2000 network, a network of preserved areas designated to protect a number of habitats and species representative of European biodiversity. The four sites in Hauts-de-France and Normandie are managed by the Conservatoire d'espaces naturels of Normandie, Picardie and Nord – Pas-de-Calais and the sites in Occitanie by the CPIE Causses méridionaux. We sampled each site once a month from April to October 2016, except for the site of Riez that was sampled from May to October.

Plant-hoverfly observations and sampling

To collect information at the community level, in each site and at each session we realized: (i) a botanic inventory of the flowering species, recorded their abundances and the total flower covering in the area and (ii) a pollinator sampling using a hand net along a variable transect walk.

Flowering plants were identified at the species level. We recorded the abundances of all flowering species. At first, we estimated the total percentage of surface covered by all flowering species in the selected area. We then estimated the relative abundance of each flowering species. We used Braun-Blanquet coefficients of abundance-dominance, ranked from i to 5 (most abundant coefficient class) (Van Der Maarel 1975, 1979; Mucina *et al.* 2000), to rank flowering species. We converted the coefficients to percentage intervals and then in mean values of percentage cover classes (Table S1): coefficient ***5*** = 75-100%, coeff ***4*** = 50-75%, coeff ***3***=25-50%, coeff ***2*** = 10-25%, coeff ***1*** = 1-10%, coeff ***+*** = few individuals less than < 1%, coeff ***i*** = 1 individual. All inventories were realized by the same surveyors to avoid biases.

Pollinator observations were performed by the same team of 3-5 persons each day. The surveyors walked slowly around any potential attractive resource patch included in the selected 1-hectare area for 4h each day. We split the sampling period into 2 hours in the morning (about 10-12h) and 2 hours in the afternoon (about 14-16h) to cover the daily variability of both pollinator (bees and hoverflies, which are more active in the morning than in the afternoon; D'Amen *et al.* 2013) and flower communities. Sampling took place when we had suitable weather conditions for pollinators (following

147 Westphal *et al.* 2008). We sampled all flower-visiting insects and we recorded observed interactions.
148 All sampled insects were immediately put individually in a killing vial with ethyl acetate and were later
149 prepared and pinned in the laboratory and identified at the species level by expert taxonomists. Even
150 if we collected both bees and hoverflies, in this study we focus on hoverflies only (since at the moment
151 of the study bees were not identified at the species level yet). Overall, we sampled for 41 days,
152 equivalent to about 164 hours in the field (all the surveyors collected at the same time). For all analyses
153 described here, we only used the list of visited herbaceous plant species and hoverflies which were
154 found visiting a plant. Despite their rarity and even if hoverflies are known to prefer open flowers
155 (Branquart & Hemptinne 2000), we also considered the interactions between hoverflies and plant
156 species of the Fabaceae family because we observed in the field that they visited Fabaceae species
157 that were already opened by other insects, *e.g.* by large bee species, such as *Eucera* sp. (de Manincor,
158 personal observation).

159 Plant – hoverfly networks

160 For each site, we constructed an interaction network consisting of all pairs of interacting plant and
161 insect species, pooling data from all months. A pair of species (*i*,*j*) was connected with intensity v_{ij} when
162 we recorded v_{ij} visits of insect species *i* on plant species *j* in the site. We calculated the network
163 specialization index, H2' (Blüthgen *et al.* 2006) using the `H2fun` function implemented in the
164 `bipartite` package (Dormann *et al.* 2009; R Core Team 2018). We obtained the *d*-value (Kullback-
165 Leibler divergence between the interactions of the focal species and the interactions predicted by the
166 weight of potential partner species in the overall network) and the *dmax*-value (maximum d-value
167 theoretically possible given the observed number of interactions in the network) using the `dfun`
168 function in the `bipartite` package (Dormann *et al.* 2009). We did not use the *d'* values provided by
169 this package as they sometimes yielded spurious results based on the computation of the minimal *d*
170 value (e.g. reporting low *d'* for species with only one partner in the network).We then manually

171 calculated the standardized specialization index *d'* (Blüthgen *et al.* 2006) for each plant and insect
172 species as the ratio of the *d*-value to its corresponding *dmax*-value.

173 We calculated the modularity of the network and the associated partition of species into modules
174 using the `cluster_leading_eigen` method for modularity optimization implemented in the
175 `igraph` package (Csardi & Nepusz 2006; Newman 2006). Modularity optimization can help identify
176 strong, simple divisions of a network into relatively independent sub-networks by looking for highly
177 interconnected sub-networks. However, modules are not meant to inform about more subtle
178 groupings among the species, *e.g.* particular avoidance of interactions between insects of group A and
179 plants of group 1. In order to detect such groups, we implemented latent block models (LBM) using
180 the `BM_poisson` method for Poisson probability distribution implemented in the `blockmodels`
181 package (Leger *et al.* 2015). Blocks are calculated separately for the two groups (insect and plant) based
182 on the number of visits (*i.e.* a weighted network). The algorithm finds the best divisions of insects and
183 plants through fitting one Poisson parameter in each block of the visit matrix, thus essentially
184 maximizing the ICL (Integrated Completed Likelihood; Biernacki *et al.* 2000; Daudin *et al.* 2008). The
185 LBM script is given in Supplementary Information (Appendix S3). All analyses were performed in R
186 version 3.3.3 (R Core Team 2018).

187 Plant and hoverfly abundances and phenology overlap

188 We calculated plant abundance using information about the abundance-dominance recorded in the
189 field following the methodology of Braun-Blanquet presented above. We transformed the coefficients
190 of abundance in percentages (Table S1): we used the mean of the percentage corresponding to each
191 class. We then calculated the relative abundance (A_P) of each flowering plant species as the ratio of
192 the focal species cumulated abundance to total flower abundance during its flowering season. For
193 hoverflies, we used the recorded number of visiting individuals (total abundance) and their presence
194 (recorded months) along the season to calculate their average abundance during months when they
195 were present (A_H).

We refer to plant phenology as their flowering period and insect phenology as the flying period. We considered only flowering plants which had been visited by pollinators. For the pollinators, we considered only hoverflies which were found in interaction. To build the species phenology tables for both plants and hoverflies, we merged the information provided by two sources of data (field data and the literature): we used the observed phenology of both plants and insects during the field session as the only source of information for plants (plants visited by insects and plants found in the botanic inventory in the site at that date), and we complemented the hoverfly phenology with information provided by the Syrph the Net Database (Speight *et al.* 2016). We then built the phenology overlap (PO) matrix based on the species phenology tables by calculating the number of phenologically active months that are shared by each pair of insect and plant species along the season.

Bayesian Structural Equation Modelling (SEM)

SEM is a confirmatory technique that involves cause-effect equations to evaluate multivariate hypotheses in ecological networks (Grace 2006). The primary interest of SEM analyses lies in its ability to compare different causal models between the same sets of explanatory and explained variables. Another important feature of SEM is that they can relate data through latent variables, *i.e.* variables which are not measured in the model and which represent underlying causes or effects, coupled with observed variables (Grace 2006; Grace *et al.* 2010). SEM can now be assessed using Bayesian approaches and parameters estimated using MCMC (Markov Chain Monte Carlo)(Grace *et al.* 2010; Fan *et al.* 2016).

In our study, we modelled hoverfly-plant interaction networks using a SEM approach (Fig. 1) with latent variables linking the number of visits per plant-pollinator species pair to abundance and phenology overlap (PO) data through a first latent table representing probabilities of interactions, another latent table representing the possible interactions between plant and pollinators (as a realization of the aforementioned interaction probability matrix), and a third latent table yielding the expected number of visits per plant-pollinator species pair (*i.e.* the intensity of interactions). We used the term latent

tables to describe latent variables organized as insect x plant tables, such as the expected number of visit matrix.

In this model, we considered that PO had an effect on possible interactions (I_{ij}) and the number of visits (λ_{ij}) – a longer overlap is intuitively expected to drive a higher probability of interaction and a larger number of visits. Interaction probabilities were also assumed to depend on two random effects (plant and insect species identities, E_i and E_j), to represent heterogeneity of species degrees (*i.e.* the number of links) in the network. We modelled the possibility of interaction I_{ij} between insect species *i* and plant species *j* (*i.e.* I_{ij} = 1 when species *i* and *j* can interact) as a Bernoulli random variable of probability μ_{ij} given by:

$$\text{logit}(\mu_{ij}) = \mu_0 + \mu_{PO} PO_{ij} + E_i + E_j$$

where logit is the usual logistic transformation (log(x/(1-x)), μ_0 is the intercept of this relation, μ_{PO} is the coefficient measuring the effect of PO, and E_i and E_j are the random effects associated with insect species i and plant species j respectively.

The number of visits V_{ij} was assumed to depend on plant and hoverfly abundances, as more abundant species are expected to be more often sampled (and thus more often recorded "in interaction"). Please note that we only linked abundances to the number of visits, V_{ij}, and not to the possibility of interaction I_{ij}, because the aim of the latter latent table is to capture "forbidden links", while detectability and sampling effects are supposed to be captured by the statistical model of the number of interactions. We integrated species abundances as predictor variables in order to assess the effect of PO on the number of visits on top of a "null model" that already includes sensible drivers of the numbers of visits, such as species abundances. V_{ij} was modelled as a Poisson random variable to allow for sampling variability, with a conditional mean λ_{ij} (the intensity of visits that can occur) given by:

$$\log(\lambda_{ij}) = \lambda_0 + \lambda_H A_{H,i} + \lambda_P A_{P,j} + \lambda_{PO} \log(1 + PO_{ij})$$

where λ_0 is the intercept of this relation, λ_H is the coefficient measuring the effect of hoverfly abundance A_H, λ_P is that of plant abundance A_P, and λ_{PO} is the coefficient of the effect of PO.

Possible interactions (I_{ij}) and the intensity of visits (λ_{ij}) are multiplied to obtain the unconditional mean number of recorded visits, *i.e.* V_{ij} is then obtained as a Poisson draw of mean $I_{ij}\,\lambda_{ij}$.

Overall we estimated four main parameters: the effect of phenology overlap on the probability of interaction ($PO \rightarrow I_{ij}$, μ_{PO}), the effect of phenology overlap on the intensity of interactions ($PO \rightarrow \lambda_{ij}$, λ_{PO}), the effect of plant abundance on the intensity of interactions ($A_P \rightarrow \lambda_{ij}$, coefficient λ_P) and the effect of insect (hoverflies) abundance on the intensity of interactions ($A_H \rightarrow \lambda_{ij}$, λ_H).

We used the `jags` function (`R2jags` package), which provides an interface from R to the JAGS library for Bayesian data analysis, to estimate model parameters. JAGS (Plummer 2003) uses a Markov Chain Monte Carlo algorithm to generate samples from the posterior distribution of the parameters. We ran two Markov chains with 10^6 iterations per chain to check for model convergence. The code of the model is given in Supplementary Material (Appendix S1 and S2).

Model and parameter comparison

We estimated the 16 models that included all combinations of 0 and 4 of the above-mentioned effects to understand which effects were more likely to play a role in the structuring of the network. The goodness-of-fit of these models were compared using the leave-one-out cross-validation criterion (LOO) calculated using the R package `loo` using Pareto smoothed importance sampling for regularizing importance weights (Vehtari *et al.* 2017). The LOO criterion is a fully Bayesian method to compare models of different complexities and to estimate prediction accuracy using the log-likelihood evaluated at the posterior simulations of the parameter values (Vehtari *et al.* 2017). Models can thus be ranked according to their LOO scores, with the best model being the one with the lowest LOO value. The LOO criterion is analogous to the classic Akaike and Bayesian Information Criteria, which are used to compare frequentist models, but can instead be applied to Bayesian models, without suffering the

instability issues of the Deviance Information Criterion which used to be the main information criterion for Bayesian models(Vehtari *et al.* 2017). To rank the models, we then calculated the *ΔLOO* (noted Δ_i) as $\Delta_i = LOO_i - LOO_{min}$ (following Burnham & Anderson 2004), where LOO_{min} is the minimum of the LOO_i values among the 16 models. We used Δ_i to obtain model weights ω_i, following the Akaike weight methodology (Burnham & Anderson 2002):

$$\omega_i = \frac{e^{-\Delta_i/2}}{\sum e^{-\Delta_i/2}}$$

We then summed weights (w_H) over all models that incorporated a given focal parameter to ascertain the plausibility of the effect associated to this parameter. We used this sum to evaluate the null hypothesis (H0) that a given factor has no effect on the plant-pollinator interactions by comparing the sum of weights to null expectations, based on the fact that each tested effect is incorporated in exactly half of the tested models. The effect is considered *plausible* when $w_H > 0.5$, *implausible* otherwise, *likely* when $w_H > 0.73$, and *unlikely* when it corresponds to a value of 0.27 or lower, following Massol *et al.* (2007).

Predictive power analysis

We tested the predictive power of the models we built by making predictions for the I_{ij} table and checking their validity using a binarized version of the visit table V_{ij}. Predictions were obtained by defining a threshold on interaction probability μ_{ij}: values found above the threshold were predicted as occurring interactions, values below the threshold as no interaction. The threshold probability value was found by maximizing the sum of model specificity and sensitivity. We computed accuracy statistics (sensitivity, specificity, omission rate, area under the ROC curve [AUC]) in two situations: (i) when predicting data for the site that was used to build the model (self-validation; e.g. predicting interaction data in the site of Riez based on the model developed for this site) and (ii) when predicting data for the other site from the same region (cross-validation; e.g. predicting data for the LAR site based on the model for the R site). We performed theses analyses using the `SDMTools` package in R. We only used

292 the set of best models (LOO < 4) found for each site to predict the interactions in the other site through
293 a multimodel averaging approach. We obtained the threshold probability using `optim.tresh`
294 function with option `max.sensitivity+specificity`.

295 **RESULTS**

296 Plant-hoverfly networks and phenology overlap

297 At the end of the field campaign we had collected 1584 hoverflies and recorded 1668 interactions
298 between 76 hoverfly species and 117 plant species overall (Table 1). The number of sampled hoverfly
299 and plant species varied between sites and among regions. In Normandie we generally sampled a
300 higher number of hoverflies than in the other two regions (Table 1) and the maximum number of visits
301 recorded in the site of FAL was 47 (between *Helophilus pendulus* and *Scabiosa columbaria*, Fig. S3) and
302 in the site of CG was 22 (between *Eristalis tenax* and *S. columbaria* and between *Sphaerophoria scripta*
303 and *Leontodon hispidus*, Fig. 3). We observed the highest diversity of both plants and hoverflies in
304 Occitanie and the lowest diversity of hoverflies in Hauts-de-France. Despite the high species diversity
305 in Occitanie, the total number of interactions recorded in these sites (BF and F) is not the highest
306 recorded in the field (Table 1): the maximum number of visits in the site of BF was 10 (between
307 *Spherophoria scripta* and *Helichrysum stoechas*, Fig. S2) and 12 in the site of F (between *Syrphus ribesii*
308 and *Bellis perennis*, Fig. 2). In the two southern sites we also recorded the lowest connectance values
309 (BF: 0.07 and F: 0.08) of all six sites, with the highest connectance observed in the site of R (R 0.16; LAR
310 0.13; CG 0.13; FAL 0.12). The maximum number of visits recorded in the site of LAR was 12 (between
311 *Syrphus ribesii* and *L. hispidus*, Fig. S4) and in the site of R was 17 (between *Syritta pipiens* and *Asperula*
312 *cynanchica*, Fig. S5).

313 In spite of differences in diversity and the number of interactions, the overall level of specialization (H2
314 index) did not show a high variation among the 6 networks (range: 0.32 – 0.37). However, we found
315 that the sites in Occitanie (BF and F) had a higher average degree of specialization (d') for both insect
316 (BF 0.63 and F 0.57) and plant species (BF 0.58 and F 0.48). The sites in Occitanie also had a higher

317 modularity (BF 0.51 and F 0.48) than the ones in Normandie (CG 0.34 and FAL 0.23) and Hauts-de-
318 France (LAR 0.37 and R 0.34; Table 1). Given that these statistics only compare 6 sites, none of these
319 assessments can be properly statistically tested, but the importance of the differences among sites is
320 highly suggestive of a difference in average specialization and modularity. We found that plant
321 phenology is generally shorter in all sites than that of hoverflies (Table 1). The phenology overlap was
322 shorter in Occitanie (BF and F) than in the other sites (Table 1).

323 Illustrations of the block clustering provided by the LBM analysis (Latent Block Model) are shown in
324 Fig. 2 and 3 in the main text and in Fig. S2 to S5 in Supplementary Information. We found different
325 numbers of blocks in plants and hoverflies among sites: the BF site had 2 insect blocks and 2 plant
326 blocks (Fig. S2); the F site had 4 of both (Fig. 2); the CG and R sites had 3 blocks for the plants and 4
327 blocks for the insects in (Fig. 3 and S5); the FAL site had 4 plant blocks and 3 insect blocks (Fig. S3); the
328 LAR site had 3 blocks for the plants and 2 for the insects (Fig. S4).

329 Model ranking and comparison of parameters in each site

330 For each site we compared the 16 models using the LOO criterion (Table 2, ΔLOO values). We found
331 that models 1, 2 and 4 had consistently better goodness-of-fit than the others. The model
332 incorporating all effects except the effect of phenological overlap on the probability of interaction
333 (Model 4: $\lambda_{ij} \sim A_H + A_P + PO$, Table 2) was the best model in the sites of CG, FAL and LAR. In the two
334 southern sites (BF and F), we found that the model incorporating all effects except that of phenological
335 overlap on the intensity of visits (Model 1: $\lambda_{ij} \sim A_H + A_P$ / $I_{ij} \sim PO$, Table 2), was the best one. The model
336 incorporating all effects (Model 0: $\lambda_{ij} \sim A_H + A_P + PO$ / $I_{ij} \sim PO$, Table 2) was found as the best one only in
337 the site of R, but was a suitable model (ΔLOO <4) in all the other sites (Table 2). We also compared the
338 sum of model weights of the four parameters among sites (Table 2, Effects weight). We found that the
339 effect of insect abundance on the intensity of interaction ($A_H \rightarrow \lambda_{ij}$) is always likely (*i.e.* the sum of their
340 weights is always higher than 0.73, Table 2) and of large effect size in all sites (standardised coefficient
341 higher than 1, Fig. 4). Likewise, we found that the effect of plant abundance on the intensity of

342 interaction ($A_P \rightarrow \lambda_{ij}$) was always likely and had large effect size in most part of sites, except in the site
343 of F (w_H = 0.59, Table 2; standardised coefficient = 0.67, Fig. 4). The effects of phenological overlap on
344 the probability of interaction (PO → I_{ij}) and the intensity of visits (PO → λ_{ij}), however, had variable
345 plausibility among sites. The effect of phenological overlap on the probability of interaction was *likely*
346 only in half of the sites (Table 2 and Fig. 4). The effect of phenological overlap on the intensity of visits
347 was *not plausible* only in the two southern sites (BF and F) and *plausible* in the other four sites (LAR, R
348 CG and FAL, Table 2 and Fig. 4). In all sites, the standardised coefficients of PO effects were always less
349 than 1, thus showing a low effect size of phenology on interaction probability and intensity (Fig. 4).

350 When assessing the predictive power of the best models, we observed that the sensitivity and
351 specificity values, both for the self-validation and the cross-validation, were higher than 0.5 (Table S2),
352 which means that the interactions predicted by the models are better than predicted by chance. While
353 area under the curve (AUC) values were all higher than 0.75 for self-validation, cross-validation tests
354 yielded intermediate values (AUC between 0.62 and 0.73), reflecting the fact that abundances and
355 phenology are certainly not sufficient to make accurate predictions on the occurrence of plant-
356 pollinator interactions.

357 **DISCUSSION**

358 Latitude affects the seasonality, with advancing species phenologies at higher latitudes, and thus, can
359 be a limiting factor for the phenological coupling of interacting species (Post *et al.* 2018). In this study
360 we explored the effect of phenology overlap on a large network of species interactions in calcareous
361 grasslands and how this effect could vary along a latitudinal gradient in France using empirical data on
362 six plant-hoverfly networks. We identified plants and insects at the species level to build detailed
363 interaction networks and hence avoid spurious generalisation levels. In order to better understand the
364 determinants of variation in species interactions in space and time, we used the latitudinal gradient to
365 consider variations linked to environmental cues and the entire flowering period to allow for seasonal
366 variation (Valverde *et al.* 2016; Pellissier *et al.* 2017). One of the main problems of comparing networks

along gradients is the dependence of network metrics on network size (Staniczenko *et al.* 2013; Astegiano *et al.* 2015; Tylianakis & Morris 2017). In this study, to avoid the problem of comparing networks with different dimensions, we decided to focus on the determinants of the probability of interaction and the number of visits, rather than the overall structure. We employed Bayesian Structural Equation Models (SEM) which is an emergent approach increasingly used to investigate complex networks of relationship in ecological studies (Grace *et al.* 2010; Eisenhauer *et al.* 2015; Fan *et al.* 2016; Theodorou *et al.* 2017). In our study we used SEM to link the numbers of visits to phenology overlap (PO) and species abundance through latent probabilities of species interaction and expected numbers of visits per plant-pollinator species pair. We tested different models with variable numbers of effects and compared them in each site. In our models, we used species abundances to construct a sensible null model to test whether phenology overlap could help explain the probability and intensity of interactions when the effects of species abundances are already taken into account. In all sites, we found that models that included both PO and abundances had always better goodness-of-fit than models that included only abundances. Abundances indeed provided a sensible null model since the goodness-of-fit of models that did not include abundances were always quite worse than the ones which did.

We also found that in all sites the most important factor affecting pollinator visits was insect abundance (Table 2). Likewise, we found that plant abundance was also a very important effect in most sites, except in the site of F (Table 2). Since insect abundances are given by visitation data, it is not surprising that the intensity of interactions positively depends on these abundances. Species abundance often explain the linkage level in pollination network studies (Olesen *et al.* 2008; Bartomeus *et al.* 2016; Chacoff *et al.* 2017; Pellissier *et al.* 2017) but it is often associated with the length of the phenology to better assess the general properties of the interaction network (Vázquez *et al.* 2009; Olito & Fox 2015). In accordance with this verbal prediction, we indeed found that the best models

incorporated the effect of PO on either the probability or the intensity of interactions (Table 2), and the model that only considered species abundance (model 5 in Table 2) was not the best one in any site. Phenology overlap generally cannot predict the probability of interaction on its own (Encinas-Viso *et al.* 2012; CaraDonna *et al.* 2017). Our findings do agree with this general predicament since no site favoured a model that only incorporated PO effects and because these effects always display lower effect sizes than the other variables. However, our objective was not to compare the effect of phenology overlap to that of species abundance – for such an endeavour, one would need estimates of species abundances independent of visitation data. Because models which consider the effect of PO on the intensity and/or probability of interactions are the best models for all sites evinces a clear effect of PO. In our model, the effect of PO on the probability of interaction and the expected number of visits also vary along the latitudinal gradient (Fig. 4).In general, we observed that southern sites (BF and F) showed shorter plant phenology and phenology overlap (PO) than the other four sites (Table 1). In these sites, plant species richness is higher and fewer visits were sampled, probably because the presence of specialist species with short phenophases may increase the number of forbidden or undetected links (Olesen *et al.* 2011; Martín González *et al.* 2012). Conversely, in sites where plant phenology is longer, PO is longer too, as observed in Normandie and Hauts-de-France (CG, FAL, LAR and R, Table 1). Moreover, when plant richness and specialization are lower, a higher number of visits can be observed (Table 1) because generalist species could interact without constraints. Indeed, in Normandie and Hauts-de-France we found that the effect of phenology overlap on the intensity of visits was always likely (PO $\rightarrow \lambda_{ij}$, Table 2) and we observed higher numbers of interactions in the first two/three blocks of insects and plants which also corresponded to blocks with longer PO (Fig. 3, S3, S4 and S5). A higher phenological overlap is expected to drive a higher probability of interactions and a larger number of visits (Olesen *et al.* 2011). In Occitanie, we did not find any effect of PO on the number of visits because the more densely visited blocks do not correspond to those with longer phenology overlap. Plant phenology can therefore drive the probability and the intensity of interactions in networks in which plant phenology is shorter, thus suggesting that hoverflies may undergo selection

418 for behavioural flexibility in order to maintain synchrony with their foraging resources (Iler *et al.* 2013;
419 Ogilvie & Forrest 2017).

420 We also found that modularity decreased along the latitudinal gradient, with richer sites (BF and F)
421 displaying higher modularity (as in Sebastián-González *et al.* 2015) but also the lower connectance. In
422 the two southern sites, higher modularity could be related to shorter phenologies and higher
423 proportions of non-overlapping sets of species, which induce some form of temporal short-term
424 specialisation (Lucas *et al.* 2018). However, modularity also seems to be influenced by species
425 abundances and degrees (Schleuning *et al.* 2014), and is expected to increase with link specificity
426 (Morente-López *et al.* 2018). Indeed, in these sites, species blocks match species degrees (Fig. 2 and
427 S2), with generalist and specialist species forming separate blocks among both plants and insects
428 (Martín González *et al.* 2012). With lower modularity and more generalist species, we expect a stronger
429 relationship between phenology and the intensity of interactions because interactions are less
430 influenced by insect preferences and more by seasonal rhythm and flower availability (Dormann *et al.*
431 2017). Thus, different phenophases might correspond to different compartments (Martín González *et*
432 *al.* 2012; Morente-López *et al.* 2018), as observed in CG, FAL, LAR and R where higher overlap
433 corresponded to higher numbers of observed visits. Although phenology improved model fit (Table 2),
434 its effect size was modest (Fig. 4), which suggests that other types of data such as traits and phylogenies
435 might help predict specific interactions. In our study, we did not consider competition among studied
436 insect species or with other group of insects, such as bees which were present in all sites. Different
437 types of pollinators with different abundances could have context-dependent effects on network
438 topology (Valverde *et al.* 2016). Moreover, in our study we only considered as "true absence" of the
439 interaction the lack of phenological coupling between species (*i.e.* plant and hoverfly species which are
440 not present at the same moment along the season cannot interact). We did not consider "false
441 absences", *i.e.* missing links, since not all the potential links among species are recorded in the field
442 (Olesen *et al.* 2011) which may introduce bias in the estimation of the probability of interactions
443 (Bartomeus *et al.* 2016; Cirtwill *et al.* 2019).

To conclude, plant phenology here drives the duration of the phenology overlap between plant and hoverflies, which in turn influences either the probability of interaction or the expected number of visits, as well as network compartmentalization. Longer phenologies correspond to less constrained interactions (lower modularity), shorter phenologies to more constrained interactions (higher modularity), which in turn restrict the number of visits. Phenology overlap alone was not sufficient to explain interactions, as suggested elsewhere (CaraDonna *et al.* 2017). Plant and insect abundances played a substantial role to explain the number of visits (as in Chacoff *et al.* 2017) since abundances may affect partner choice (Trøjelsgaard *et al.* 2015). Our results, and the ability of the method used here to compare different effects on interaction patterns, suggest that the use of Bayesian SEM to compare networks of different sizes is a valuable tool which can help understand plant-pollinator networks (Eisenhauer *et al.* 2015). The use of latent variables can help predict the probability of interaction and the expected number of visits while avoiding circularity – the introduction of plant and insect specific random effects played the role of an implicit "degree" effect. Our results demonstrate the importance of considering differences in plant and insect phenologies to better predict their interactions in pollination networks at different latitudes. The use of morphological traits (*e.g.* tongue length, inter-tegular distance, …) together with species richness and phylogenies, on top of variables already used, might improve the modelling of interactions and could help better understand some forbidden or missing links in richer communities or considering other pollinators (*e.g.* wild bees).

ACKNOWLEDGEMENTS

Financial support was provided by the ANR ARSENIC project (grant no. 14-CE02-0012), the Region Nord-Pas-de-Calais and the CNRS. We also thank Martin Speight for insect identification, Clément Mazoyer for informatic support and all the students who took part in the field campaign. This work is a contribution to the CPER research project CLIMIBIO. The authors thank the French Ministère de l'Enseignement Supérieur et de la Recherche, the Hauts-de-France Region and the European Funds for Regional Economical Development for their financial support.

470

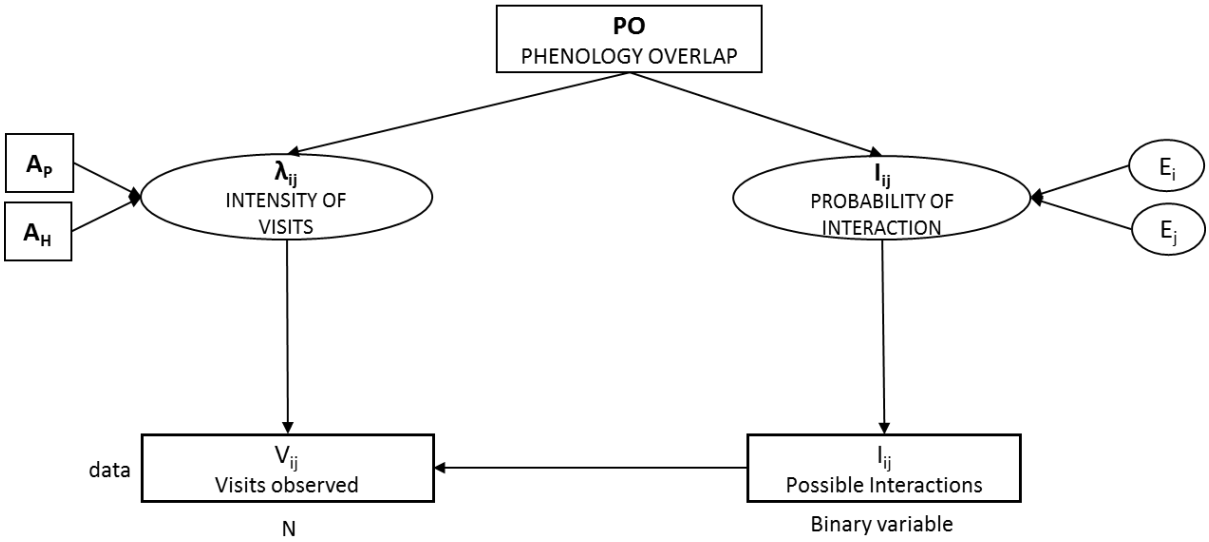

Figure 1. Summary diagram of the SEM model. We estimated 4 effects: the effect of plant abundance (AP → λij, coefficient λP), the effect of insect (hoverflies) abundance on the intensity of visits (AH → λij, λH), the effect of phenology overlap on the intensity of visits (PO → λij, λPO) and the effect of phenology overlap on the probability of interaction (PO → Iij, μPO). The phenology overlap (PO) is the number of phenologically active months that are shared by each pair of insect and plant species along the season. The intensity of visits (λij) and the probability of interaction are latent variables in the model. Effect-i and effect-p are random effects calculated by the model which represent the insect and plant species identities. The Iij (Possible interactions) is a binary variable and the Vij (visits observed) follow a Poisson distribution with an expected value given when the probability of interaction is predicted as "true". Rectangles represent observed variables while ovals represent unobserved influences.

Figure 2. Block clustering provided by LBM in the site of Fourches (F, Occitanie), overlaid on a heatmap of species phenology overlap. The LBM algorithm finds the best division for the group of insects and plants independently through fitting Poisson parameters in each block maximizing the likelihood (ICL). Insect species are displayed in rows and plant species in columns, following their degree (number of partners). The blocks of insects and the blocks of plants are separated by solid black lines. Colours correspond to the number of months that are shared by each pair of plant and insect species (PO, phenology overlap), with higher PO corresponding to darker colours. Numbers are the number of visits observed in the field for a given plant-insect pair.

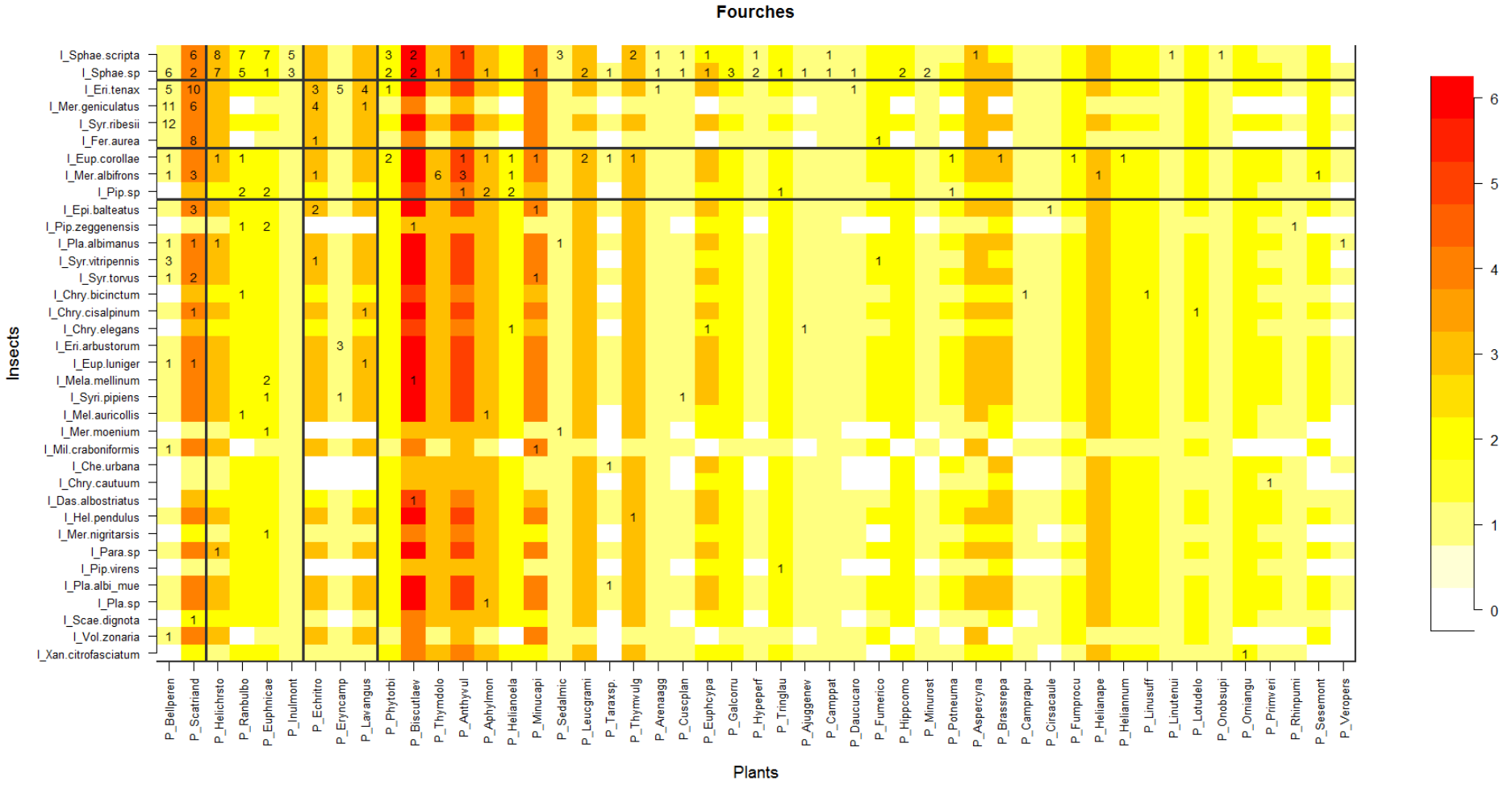

Figure 3. Block clustering provided by LBM in the site of Chateau Gaillard (CG, Normandie) overlaid on a heatmap of species phenology overlap. Insect species are displayed in rows and plant species in columns, following their degree (number of partners). The blocks of insects and the blocks of plants are separated by solid black lines. Colours correspond to the number of months that are shared by each pair of plant and insect species (PO, phenology overlap), with higher PO corresponding to darker colours. Numbers are the number of visits observed in the field for a given plant-insect pair.

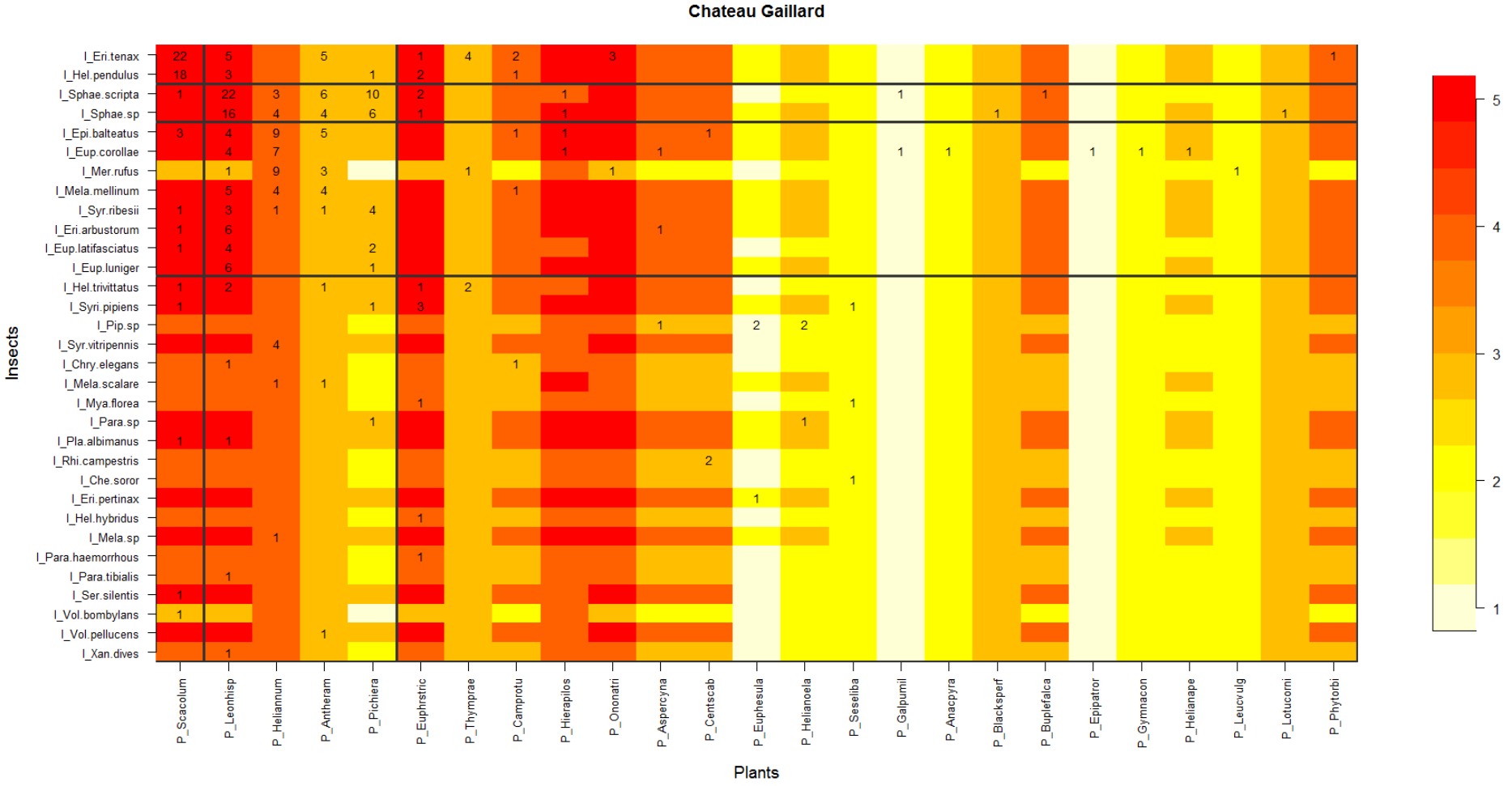

Figure 4. Summary diagram of the best models in all sites. The thickness of the arrows is scaled to Akaike weights (thin ER < 0.73; thick ER > 0.73, cf. Table 2). Standardised coefficients of the model average (computed based on the Akaike weighted model average) are reported next to the arrows. PO is the phenology overlap, I_{ij} is the probability of interaction, λ_{ij} is the intensity of visits, A_H and A_P are the hoverflies and plant abundances respectively.

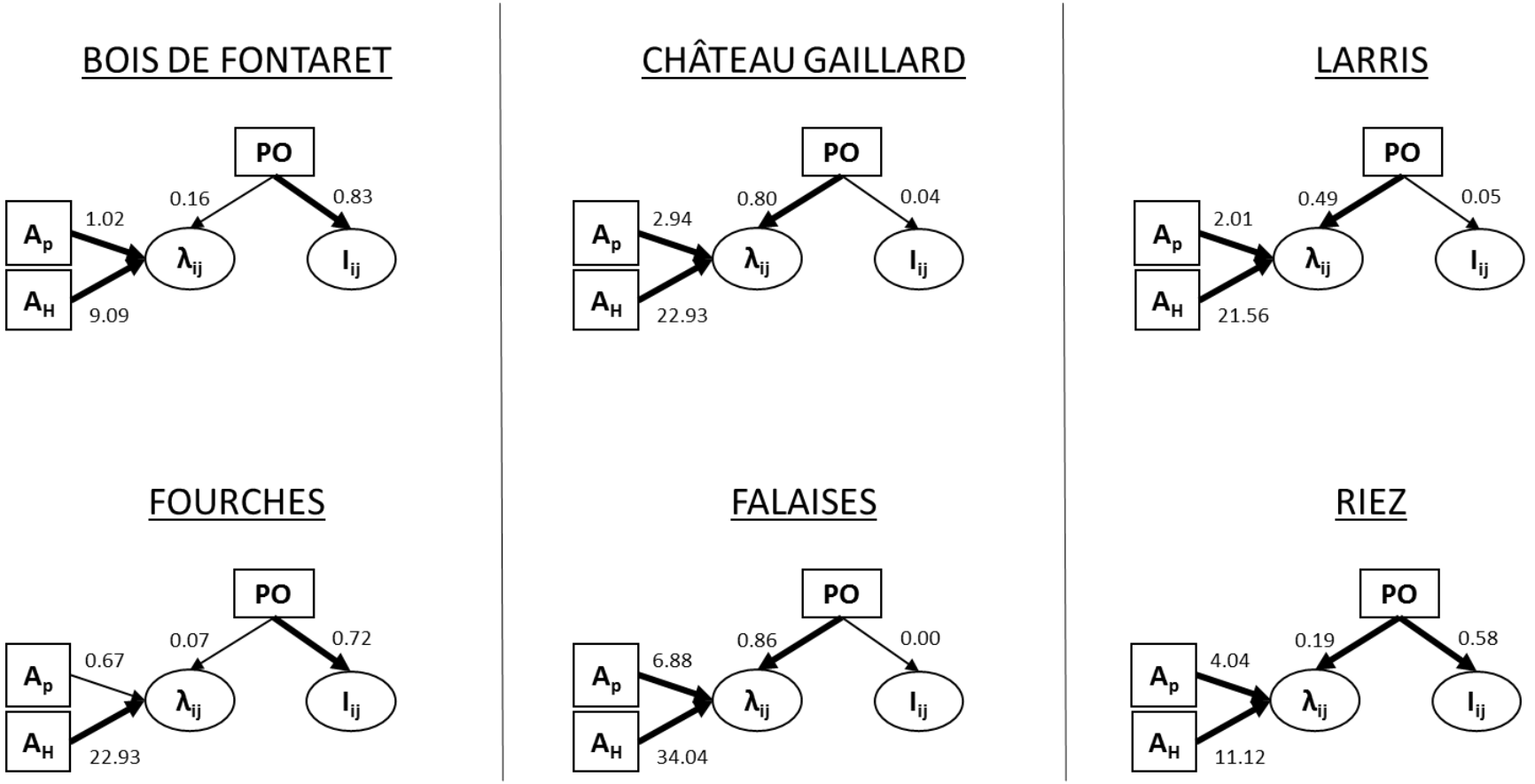

Table 1. Summary table of results obtained in each site (Bois de Fontaret [BF] and Fourches [F] in Occitanie, Château Gaillard [CG] and Falaises [FAL] in Normandie, Larris [LAR] and Riez [R] in Hauts-de-France). `H2'` and `d'` indices refer to specialization indices described by Blüthgen *et al.* (2006) and implemented in the R package `bipartite` (Dormann *et al.* 2009). The modularity score was obtained using the `leading-eigenvector` method described by Newman (2006) and implemented in the `igraph` package (Csardi & Nepusz 2006). LBM refers to latent block modelling as implemented in the R package `blockmodels` (Leger *et al.* 2015).

		Collected data				Specialization index			Species phenology			Modularity analysis	LBM	
Site	Region	Sampled insects	Insect species	Plant species	Recorded Interactions	H2' index	d' Insects (average + sd)	d' Plants (average + sd)	Insect (average + sd)	Plant (average + sd)	Phenology overlap (PO) (average + sd)	modularity score	blocks I	blocks P
BF	Occitanie	197	40	43	198	0.37	0.63 ± 0.17	0.58 ± 0.17	5.25 ± 1.51	2.14 ± 1.04	1.77 ± 1.03	0.53	2	2
F	Occitanie	223	36	49	286	0.33	0.57 ± 0.18	0.48 ± 0.19	5.61 ± 1.54	2.08 ± 1.13	1.78 ± 1.14	0.48	4	4
CG	Normandie	295	32	25	297	0.34	0.40 ± 0.21	0.47 ± 0.18	6.03 ± 1.00	3.28 ± 1.24	3.02 ± 1.17	0.34	4	3
FAL	Normandie	363	34	30	374	0.32	0.40 ± 0.18	0.41 ± 0.18	6.06 ± 1.13	3.57 ± 1.59	3.23 ± 1.51	0.23	3	4
LAR	Hauts-de-France	220	24	33	220	0.36	0.48 ± 0.19	0.45 ± 0.15	6.38 ± 0.82	3.18 ± 1.38	2.99 ± 1.36	0.37	2	3
R	Hauts-de-France	286	22	29	293	0.32	0.39 ± 0.16	0.40 ± 0.16	5.55 0.74	3.38 ± 1.47	3.11 ± 1.45	0.34	4	3
	Total	**1584**	**76**	**117**	**1668**									

Table 2. (i) Comparison of SEM models using the leave-one-out cross-validation criterion (LOO); (ii) evidence ratios (ER) of model effects in each site. (i) Models are ranked depending on the number of parameters used (from 0 to 4). The best models are the ones with ΔLOO=0 (underlined and bold values). The other suitable models are the ones with ΔLOO <4 (underlined and italic values). λ_{ij} is the intensity of visits, I_{ij} is the probability of interaction, A_H is the insect abundance, A_P is the plant abundance and PO is the phenology overlap. (ii) We compared 4 model effects: PO → I_{ij}, effect of the phenology overlap on the probability of interaction; PO → λ_{ij} effect of the phenology overlap on the intensity of visits; A_H → $\boldsymbol{\lambda_{ij}}$ and A_P → $\boldsymbol{\lambda_{ij}}$ effects of the hoverflies and plant abundances on the intensity of interaction. The w_H limits for unlikelihood is 0.27, plausibility 0.5 and likelihood 0.73. Underlined and bold values represent the likely hypothesis only.

			Sites					
			BF	F	CG	FAL	LAR	R
Model		*Nb of parameters*	*ΔLOO values*					
0	**λ_{ij} ~ A_H + A_P + PO / I_{ij} ~ PO**	4	*2.98*	*2.04*	*3.54*	*2.54*	*2.86*	**0.00**
1	**λ_{ij} ~ A_H + A_P / I_{ij} ~ PO**	3	**0.00**	**0.00**	36.75	64.04	10.37	*2.90*
2	λ_{ij} ~ A_P + PO / I_{ij} ~ PO	3	8.66	78.23	106.46	184.02	44.60	17.00
3	λ_{ij} ~ A_H + PO / I_{ij} ~ PO	3	6.63	*1.71*	8.09	73.62	11.24	11.42
4	**λ_{ij} ~ A_H + A_P + PO**	3	*2.86*	8.06	**0.00**	**0.00**	**0.00**	*2.24*
5	λ_{ij} ~ PO / I_{ij} ~ PO	2	14.69	73.20	109.85	223.86	55.67	23.09
6	λ_{ij} ~ A_H / I_{ij} ~ PO	2	*1.45*	*1.31*	33.53	119.04	27.23	19.76
7	λ_{ij} ~ A_P / I_{ij} ~ PO	2	9.84	72.16	156.61	256.04	47.99	21.53
8	λ_{ij} ~ A_H + PO	2	11.49	8.18	5.25	71.97	10.28	13.80
9	λ_{ij} ~ A_P + PO	2	10.71	88.67	103.46	182.14	44.36	17.94
10	λ_{ij} ~ A_H + A_P	2	24.36	14.04	36.10	66.82	10.51	4.26
11	I_{ij} ~ PO	1	11.78	68.52	154.26	272.98	64.12	32.39
12	λ_{ij} ~ PO	1	19.99	86.20	108.46	219.66	54.64	25.73
13	λ_{ij} ~ A_H	1	25.58	14.41	36.12	123.30	28.27	22.78
14	λ_{ij} ~ A_P	1	32.99	87.70	157.74	256.39	48.82	22.87
15	-	0	34.39	83.89	155.68	274.80	64.78	33.52
Model effects			Effects weight (w_H)					
	PO → I_{ij}		**0.88**	**0.98**	0.15	0.22	0.20	**0.74**
	PO → λ_{ij}		0.26	0.35	**1.00**	**1.00**	**0.99**	**0.79**
	A_H → λ_{ij}		**0.99**	**1.00**	**1.00**	**1.00**	**1.00**	**1.00**
	A_P → λ_{ij}		**0.74**	0.59	**0.93**	**1.00**	**0.99**	**1.00**

519 **Supporting Information**

520 The following Supporting Information is available for this article:

521 Appendix S1. Model code.

522 Appendix S2. Model script for the 16 models.

523 Appendix S3. Script modularity and latent block model analysis (LBM).

524 Figure S1. Sites location in France.

525 Figure S2. Block clustering provided by LBM in the site of Bois de Fontaret (BF, Occitanie), overlaid on
526 a heatmap of species phenology overlap.

527 Figure S3. Block clustering provided by LBM in the site of Falaises (FAL, Normandie), overlaid on a
528 heatmap of species phenology overlap.

529 Figure S4. Block clustering provided by LBM in the site of Larris (LAR, Hauts-de-France), overlaid on a
530 heatmap of species phenology overlap.

531 Figure S5. Block clustering provided by LBM in the site of Riez (R, Hauts-de-France), overlaid on a
532 heatmap of species phenology overlap.

533 Table S1. Table of transformed plant abundances.

534

535 REFERENCES

536 Astegiano, J., Massol, F., Vidal, M.M., Cheptou, P.O. & Guimarães, P.R. (2015). The robustness of
537 plant-pollinator assemblages: Linking plant interaction patterns and sensitivity to pollinator
538 loss. *PLoS One*, 10, e0117243.

539 Bartomeus, I., Ascher, J.S., Wagner, D., Danforth, B.N., Colla, S., Kornbluth, S., *et al.* (2011). Climate-
540 associated phenological advances in bee pollinators and bee-pollinated plants. *Proc. Natl. Acad.*
541 *Sci. U. S. A.*, 108, 20645–9.

542 Bartomeus, I., Gravel, D., Tylianakis, J.M., Aizen, M.A., Dickie, I.A. & Bernard-Verdier, M. (2016). A
543 common framework for identifying linkage rules across different types of interactions. *Funct.*
544 *Ecol.*, 30, 1894–1903.

545 Baude, M., Kunin, W.E., Boatman, N.D., Conyers, S., Davies, N., Gillespie, M.A.K., *et al.* (2016).
546 Historical nectar assessment reveals the fall and rise of floral resources in Britain. *Nature*, 530,
547 85–88.

548 Biernacki, C., Celeux, G. & Govaert, G. (2000). Assessing a mixture model for clustering with
549 integrated completed likelihood. *IEEE Trans. Pattern Anal. Mach. Intell.*, 22, 719–725.

550 Blüthgen, N., Menzel, F. & Blüthgen, N. (2006). Measuring specialization in species interaction
551 networks. *BMC Ecol.*, 6, 9.

552 Branquart, E. & Hemptinne, J. (2000). Selectivity in the exploitation of floral resources by hoverflies
553 (Diptera: Syrphinae). *Ecography (Cop.).*, 23, 732–742.

554 Burnham, K.P. & Anderson, D.R. (2002). *Model Selection and Multimodel Inference A Practical*
555 *Information-Theoretic Approach*. 2nd Editio. Springer-Verlag, New York.

556 Burnham, K.P. & Anderson, D.R. (2004). Multimodel inference: Understanding AIC and BIC in model
557 selection. *Sociol. Methods Res.*, 33, 261–304.

558 CaraDonna, P.J., Petry, W.K., Brennan, R.M., Cunningham, J.L., Bronstein, J.L., Waser, N.M., *et al.*
559 (2017). Interaction rewiring and the rapid turnover of plant – pollinator networks. *Ecol. Lett.*,
560 20, 385–394.

561 Chacoff, N.P., Resasco, J. & Vázquez, D.P. (2017). Interaction frequency, network position, and the
562 temporal persistence of interactions in a plant–pollinator network. *Ecology*, 99, 21–28.

563 Cirtwill, A.R., Eklof, A., Roslin, T., Wootton, K. & Gravel, D. (2019). A quantitative framework for
564 investigating the reliability of network construction. *Methods Ecol. Evol.*, 10, 902–911.

565 Colley, M.R. & Luna, J.M. (2000). Relative attractiveness of potential beneficial insectary plants to
566 aphidophagous hoverflies (Diptera: Syrphidae). *Environ. Entomol.*, 29, 1054–1059.

567 Cowgill, S.E., Wratten, S.D. & Sotherton, N.W. (1993). The selective use of floral resources by the
568 hoverfly Episyrphus balteatus (Diptera: Syrphidae) on farmland. *Ann. Appl. Biol.*, 122, 223–231.

569 Csardi, G. & Nepusz, T. (2006). The igraph software package for complex network research.
570 *InterJournal*, Complex Sy, 1695.

571 D'Amen, M., Birtele, D., Zapponi, L. & Hardersen, S. (2013). Patterns in diurnal co-occurrence in an
572 assemblage of hoverflies (Diptera: Syrphidae). *Eur. J. Entomol.*, 110, 649–656.

573 Daudin, J.J., Picard, F. & Robin, S. (2008). A mixture model for random graphs. *Stat. Comput.*, 18,
574 173–183.

575 Devoto, M., Medan, D. & Montaldo, N.H. (2005). Patterns of interaction between plants and
576 pollinators along an environmental gradient. *Oikos*, 109, 461–472.

577 Dormann, C.F., Fründ, J., Blüthgen, N. & Gruber, B. (2009). Indices, graphs and null models: analyzing
578 bipartite ecological networks. *Open Ecol. J.*, 2, 7–24.

579 Dormann, C.F., Fründ, J. & Schaefer, H.M. (2017). Identifying causes of patterns in ecological
580 networks: opportunities and limitations. *Annu. Rev. Ecol. Evol. Syst.*, 48, 12–20.

581 Eisenhauer, N., Bowker, M.A., Grace, J.B. & Powell, J.R. (2015). From patterns to causal
582 understanding: Structural equation modeling (SEM) in soil ecology. *Pedobiologia (Jena).*, 58, 65–
583 72.

584 Encinas-Viso, F., Revilla, T.A. & Etienne, R.S. (2012). Phenology drives mutualistic network structure
585 and diversity. *Ecol. Lett.*, 15, 198–208.

586 Fan, Y., Chen, J., Shirkey, G., John, R., Wu, S.R., Park, H., *et al.* (2016). Applications of structural
587 equation modeling (SEM) in ecological studies: an updated review. *Ecol. Process.*

588 Fortuna, M.A., Stouffer, D.B., Olesen, J.M., Jordano, P., Mouillot, D., Krasnov, B.R., *et al.* (2010).
589 Nestedness versus modularity in ecological networks: Two sides of the same coin? *J. Anim.*
590 *Ecol.*, 79, 811–817.

591 Grace, J.B. (2006). *Structural Equation Modeling and Natural Systems*. Cambridge University Press,
592 New York.

593 Grace, J.B., Anderson, T.M., Olff, H. & Scheiner, S.M. (2010). On the specification of structural
594 equation models for ecological systems. *Ecol. Monogr.*, 80, 67–87.

595 Grace, J.B. & Bollen, K.A. (2008). Representing general theoretical concepts in structural equation
596 models: The role of composite variables. *Environ. Ecol. Stat.*, 15, 191–213.

597 Hutchings, M.J., Robbirt, K.M., Roberts, D.L. & Davy, A.J. (2018). Vulnerability of a specialized
598 pollination mechanism to climate change revealed by a 356-year analysis. *Bot. J. Linn. Soc.*, 186,
599 498–509.

600 Iler, A., Inouye, D., Høye, T., Miller-Rushing, A., Burkle, L. & Johnston, E. (2013). Maintenance of
601 temporal synchrony between syrphid flies and floral resources despite differential phenological
602 responses to climate. *Glob. Chang. Biol.*, 19, 2348–2359.

603 Jauker, F. & Wolters, V. (2008). Hover flies are efficient pollinators of oilseed rape. *Oecologia*, 156,
604 819–823.

605 Klecka, J., Biella, P. & Klecka, J. (2018a). Flower visitation by hoverflies (Diptera : Syrphidae) in a
606 temperate plant-pollinator network. *PeerJPreprints*, 19, 780–785.

607 Klecka, J., Hadrava, J. & Kolouškova, P. (2018b). Vertical stratification of plant–pollinator interactions
608 in a temperate grassland. *PeerJ*, 6, e4998.

609 Leger, J.B., Daudin, J.J. & Vacher, C. (2015). Clustering methods differ in their ability to detect
610 patterns in ecological networks. *Methods Ecol. Evol.*, 6, 474–481.

611 Lucas, A., Bodger, O., Brosi, B.J., Ford, C.R., Forman, D.W., Greig, C., *et al.* (2018). Generalisation and
612 specialisation in hoverfly (Syrphidae) grassland pollen transport networks revealed by DNA
613 metabarcoding. *J. Anim. Ecol.*, 87, 1008–1021.

614 Lunau, K. (2014). Visual ecology of flies with particular reference to colour vision and colour

preferences. *J. Comp. Physiol. A Neuroethol. Sensory, Neural, Behav. Physiol.*, 200, 497–512.

Van Der Maarel, E. (1975). The Braun-Blanquet approach in perspective. *Veget*, 30, 213–219.

Van Der Maarel, E. (1979). Arrhenatheretum, Classification, Combined estimation, Cover-abundance scale, Ordination, Phytosociology, Salt marsh, Similarity, Transformation. *Vegetatio*, 39, 97–114.

Martín González, A.M., Allesina, S., Rodrigo, A. & Bosch, J. (2012). Drivers of compartmentalization in a Mediterranean pollination network. *Oikos*, 121, 2001–2013.

Massol, F., David, P., Gerdeaux, D. & Jarne, P. (2007). The influence of trophic status and large-scale climatic change on the structure of fish communities in Perialpine lakes. *J. Anim. Ecol.*, 76, 538–551.

Memmott, J., Craze, P.G., Waser, N.M. & Price, M. V. (2007). Global warming and the disruption of plant-pollinator interactions. *Ecol. Lett.*, 10, 710–717.

Miller-Struttmann, N.E., Geib, J.C., Franklin, J.D., Kevan, P.G., Holdo, R.M., Ebert-may, D., *et al.* (2015). Functional mismatch in a bumble bee pollination mutualism under climate change. *Science*, 349, 1541–4.

Morente-López, J., Lara-Romero, C., Ornosa, C. & Iriondo, J.M. (2018). Phenology drives species interactions and modularity in a plant - flower visitor network. *Sci. Rep.*, 8, 9386.

Mucina, L., Schaminée, J.H.J. & Rodwell, J.S. (2000). Common data standards for recording relevés in field survey for vegetation classification. *J. Veg. Sci.*, 11, 769–772.

Newman, M.E.J. (2006). Finding community structure in networks using the eigenvectors of matrices. *Phys. Rev. E - Stat. Nonlinear, Soft Matter Phys.*, 74, 036104.

Ogilvie, J.E. & Forrest, J.R. (2017). Interactions between bee foraging and floral resource phenology shape bee populations and communities. *Curr. Opin. Insect Sci.*

Olesen, J.M., Bascompte, J., Dupont, Y.L., Elberling, H., Rasmussen, C. & Jordano, P. (2011). Missing and forbidden links in mutualistic networks. *Proc. Biol. Sci.*, 278, 725–732.

Olesen, J.M., Bascompte, J., Elberling, H. & Jordano, P. (2008). Temporal dynamics in a pollination network. *Ecology*, 89, 1573–1582.

Olito, C. & Fox, J.W. (2015). Species traits and abundances predict metrics of plant-pollinator network structure, but not pairwise interactions. *Oikos*, 124, 428–436.

Parmesan, C. (2007). Influences of species, latitudes and methodologies on estimates of phenological response to global warming. *Glob. Chang. Biol.*, 13, 1860–1872.

Pellissier, L., Albouy, C., Bascompte, J., Farwig, N., Graham, C., Loreau, M., *et al.* (2017). Comparing species interaction networks along environmental gradients. *Biol. Rev.*, 93, 785–800.

Plummer, M. (2003). JAGS: a program for analysis of Bayesian graphical models using Gibbs sampling.

Poisot, T. & Gravel, D. (2014). When is an ecological network complex? Connectance drives degree distribution and emerging network properties. *PeerJ*, 2, e251.

Post, E., Steinman, B.A. & Mann, M.E. (2018). Acceleration of phenological advance and warming with latitude over the past century. *Sci. Rep.*, 8, 3927.

R Core Team. (2018). R: A language and environment for statistical computing. R Foundation for Statistical Computing, Vienna, Austria. URL https://www.R-project.org/.

654 Rader, R., Edwards, W., Westcott, D.A., Cunningham, S.A. & Howlett, B.G. (2011). Pollen transport
655 differs among bees and flies in a human-modified landscape. *Divers. Distrib.*, 17, 519–529.

656 Rafferty, N.E. (2017). Effects of global change on insect pollinators: multiple drivers lead to novel
657 communities. *Curr. Opin. Insect Sci.*

658 Rafferty, N.E., CaraDonna, P.J. & Bronstein, J.L. (2015). Phenological shifts and the fate of
659 mutualisms. *Oikos*, 124, 14–21.

660 Schleuning, M., Fru, J., Klein, A., Abrahamczyk, S., Albrecht, M., Andersson, G.K.S., *et al.* (2012).
661 Report Specialization of Mutualistic Interaction Networks Decreases toward Tropical Latitudes,
662 1925–1931.

663 Schleuning, M., Ingmann, L., Strauß, R., Fritz, S.A., Dalsgaard, B., Matthias Dehling, D., *et al.* (2014).
664 Ecological, historical and evolutionary determinants of modularity in weighted seed-dispersal
665 networks. *Ecol. Lett.*, 17, 454–463.

666 Sebastián-González, E., Dalsgaard, B., Sandel, B. & Guimarães, P.R. (2015). Macroecological trends in
667 nestedness and modularity of seed-dispersal networks: Human impact matters. *Glob. Ecol.*
668 *Biogeogr.*, 24, 293–303.

669 Speight, M.C.D., Castella, E., Sarthou, J.-P. & Vanappelghem, C. (2016). StN 2016. In: Syrph the Net on
670 CD, Issue 11. Speight, M.C.D., Castella, E., Sarthou, J.-P. & Vanappelghem, C. (Eds.) Syrph the
671 Net Publications, Dublin.

672 Staniczenko, P.P.A., Kopp, J.C. & Allesina, S. (2013). The ghost of nestedness in ecological networks.
673 *Nat. Commun.*, 4, 1391–1396.

674 Staniczenko, P.P.A., Lewis, O.T., Tylianakis, J.M., Albrecht, M., Coudrain, V., Klein, A.-M., *et al.* (2017).
675 Predicting the effect of habitat modification on networks of interacting species. *Nat. Commun.*,
676 8.

677 Theodorou, P., Albig, K., Radzevičiūtė, R., Settele, J., Schweiger, O., Murray, T.E., *et al.* (2017). The
678 structure of flower visitor networks in relation to pollination across an agricultural to urban
679 gradient. *Funct. Ecol.*, 31, 838–847.

680 Trøjelsgaard, K., Jordano, P., Carstensen, D.W. & Olesen, J.M. (2015). Geographical variation in
681 mutualistic networks: Similarity, turnover and partner fidelity. *Proc. R. Soc. B Biol. Sci.*, 282,
682 20142925.

683 Tylianakis, J.M. & Morris, R.J. (2017). Ecological networks across environmental gradients. *Annu. Rev.*
684 *Ecol. Evol. Syst.*, 48, 25–48.

685 Valverde, J., Gómez, J.M. & Perfectti, F. (2016). The temporal dimension in individual-based plant
686 pollination networks. *Oikos*, 125, 468–479.

687 Vázquez, D.P., Chacoff, N.P. & Cagnolo, L. (2009). Evaluating multiple determinants of the structure
688 of plant-animal mutualistic networks. *Ecology*, 90, 2039–2046.

689 Vehtari, A., Gelman, A. & Gabry, J. (2017). Practical Bayesian model evaluation using leave-one-out
690 cross-validation and WAIC. *Stat. Comput.*, 27, 1413–1432.

691 Westphal, C., Bommarco, R., Carré, G., Lamborn, E., Morison, M., Petanidou, T., *et al.* (2008).
692 Measuring bee diversity in different European habitats and biogeographic regions. *Ecol.*
693 *Monogr.*, 78, 653–671.

694 Willmer, P. (2012). Ecology: Pollinator-plant synchrony tested by climate change. *Curr. Biol.*, 22,

695 R131–R132.
696

Supplementary Information

Does phenology explain plant-pollinator interactions at different latitudes? An assessment of its explanatory power in plant-hoverfly networks in French calcareous grasslands

N. de Manincor[1]*, N. Hautekeete[1], Y. Piquot[1], B. Schatz[2], C. Vanappelghem[3], F. Massol[1,4]

[1] Université de Lille, CNRS, UMR 8198 - Evo-Eco-Paleo, 59000 Lille, France
[2] CEFE, EPHE-PSL, CNRS, University of Montpellier, University of Paul Valéry Montpellier 3, IRD, Montpellier, France
[3] Conservatoire d'espaces naturels Nord et du Pas-de-Calais, 160 rue Achille Fanien - ZA de la Haye, 62190 LILLERS
[4] Univ. Lille, CNRS, Inserm, CHU Lille, Institut Pasteur de Lille, U1019 - UMR 8204 - CIIL - Center for Infection and Immunity of Lille, F-59000 Lille, France

Natasha de Manincor ORCID: 0000-0001-9696-125X
Nina Hautekeete ORCID: 0000-0002-6071-5601
Yves Piquot ORCID: 0000-0001-9977-8936
Bertrand Schatz ORCID: 0000-0003-0135-8154
François Massol ORCID: 0000-0002-4098-955X

*Corresponding author

E-mail adresses: natasha.de-manincor@univ-lille.fr, francois.massol@univ-lille.fr, nina.hautekeete@univ-lille.fr, yves.piquot@univ-lille.fr, Bertrand.SCHATZ@cefe.cnrs.fr, cedric.vanappelghem@espaces-naturels.fr

Appendix S1: Model Code

The model code (in JAGS language) given in this supplementary material refers to the "model Z0" which considers all four parameters (model effects, Table 2 in the main text). Overall, we estimated 16 models that included between 0 and 4 of the above-mentioned effects. To create the code for these other models, parameters should be removed following the order in the Tab. 2. The four parameters tested in the model are: (i) alpha: effect of the phenology overlap (cooc) on the probability of interaction; (ii) epsilon: effect of the phenology overlap on the intensity of visits; (iii) gamma: effect of the insect abundances (ab_I) on the intensity of visits; and (iv) delta: effect of the plant abundances (ab_P) on the intensity of visits.

```
model
{
  for( i in 1 : dim1 ) {
    for( p in 1 : dim2 ) {
      inter[i , p] ~ dbern(mu[i , p])
          logit(mu[i , p]) <- beta + alpha*cooc[i , p] + effet_I[i] + effet_P[p]
          lambda[i,p] <- exp(theta[i,p])
          theta[i,p] <- theta0 + gamma*ab_I[i] + delta*ab_P[p] + epsilon*log(1+cooc[i,p])
          visit[i,p] ~ dpois( inter[i,p]*lambda[i,p] )
          loglik[i,p] <- log(ifelse(visit[i,p]==0,1-mu[i,p]+mu[i , p]*dpois(visit[i,p],lambda[i,p]),mu[i ,
p]*dpois(visit[i,p],lambda[i,p])))
    }
  }

  for( i in 1 : dim1 ) {
    effet_I[i] ~ dnorm( 0.0,tau_I)
```

```
746       }
747
748       for( p in 1 : dim2 ) {
749         effet_P[p] ~ dnorm( 0.0,tau_P)
750       }
751
752               tau_I ~ dexp( 10)
753               tau_P ~ dexp( 10)
754               alpha ~ dnorm(0,0.01)
755               beta ~  dnorm(0,0.01)
756               theta0 ~ dnorm(0,0.01)
757               gamma ~ dnorm(0,0.01)
758               delta ~ dnorm(0,0.01)
759               epsilon ~ dnorm(0,0.01)
760     }
761
```

Appendix 2: Model script for the 16 models – LOO values

The following generic script was applied to all the study sites using all 16 models. The script is separated in three blocks which communicate among them: the script options, the model definitions and the execution (model inference). We defined three options to set (i) the name of the directory (-d), (ii) the site (-s) and (iii) the type of model (-m).

We used, as an example, the information for the site of Bois de Fontaret (BF).

Exemple: Rscript (name) “script-SEMLOO_generique.R” “-d o-BFs-2016” “-s BFs”

In order to calculate the standardised coefficients for each parameters used, at the end of the third block, we added the functions to get the parameter values for each site and each model.

```
############################### BLOCK 1 – SCRIPT OPTION ##############################
library(optparse)
option_list = list(
      make_option(c("-d", "--dir"), type="character", default=NULL, help="directory",
metavar="character"),
      make_option(c("-s", "--site"), type="character", default=NULL, help="site name",
metavar="character"),
          make_option(c("-m", "--modele"), type="character", default="all", help="modele name",
metavar="character"))
opt_parser = OptionParser(option_list=option_list);
opt = parse_args(opt_parser);
site<-opt$site
dossier<-opt$dir
################################## Librairies ##########################
library(bipartite)
library(vegan)
library(igraph)
```

```
788 library(magrittr)
789 library(dummies)
790 library(MuMIn)
791 library(rjags)
792 library(boot)
793 library(R2jags)
794 library(coda)
795 library(lattice)
796 library(ggplot2)
797 library(loo)
798 library(matrixStats)
799 ############################ Function to record the LOO values ########################
800 write_values<-function(x, f, app)
801 {
802         write.table(x, append=app, file=f, sep="\t", row.names=T, col.names=T, quote=F)
803 }
804 ############################ BLOCK 2 – MODEL FUNCTIONS ############################
805 #Model function and model initialization: one function for each model from model Z15, with 0
806 parameters, to Z00 with all the parameters#
807 ### MODEL Z015
808 mZ015<-function(){
809         init.funZ015 <-function(){
810           list("tau_I" = rexp(1,10), "tau_P" = rexp(1,10), "beta" = rnorm(1,0,1), "theta0" =
811 rnorm(1,0,1), "effet_I"=rnorm(dim1,0,1),"effet_P"=rnorm(dim2,0,1), "inter"=inter0)
812         }
```

```
813             mod.Z015<<-jags(inits=init.funZ015,model.file = "modelZ015_code.txt",data =
814 list("visit","dim1","dim2"),parameters.to.save =
815 c("mu","effet_I","effet_P","tau_I","tau_P","beta","theta0", "loglik"),n.chains = 1, n.iter=1000000,
816 n.burnin = 250000, n.thin = 250)
817             mod.Z015.mcmc<-as.mcmc(mod.Z015)
818             mZ015<-mod.Z015$BUGSoutput$sims.list
819             mZ015.deviance<-mZ015$deviance
820             mZ015.loglik<-mZ015$loglik
821             dimSEM<-dim(mZ015.loglik)[1]
822             list.mZ015<-sapply(1:dimSEM,function(x) matrix(mZ015.loglik[x,,],nrow=dim1*dim2))
823             list.tmZ015<-(t(list.mZ015))
824             mZ015.loo<-loo(list.tmZ015)
825             loo_file<-paste(dossier, "/", site, "_Z015_loo.txt", sep="")
826             write_values("mZ015", app=F, loo_file)
827             mZ015_loo_pointwise<-mZ015.loo$pointwise
828             mZ015_loo_pareto_k<-mZ015.loo$pareto_k
829             mZ015.loo$pareto_k<-NULL
830             mZ015.loo$pointwise<-NULL
831             write_values(as.matrix(mZ015.loo), app=T, loo_file)
832             save.image(paste(dossier, "/", site, "_Z015.RData", sep=""))
833 }
834 ### MODEL Z014
835 mZ014<-function(){
836             init.funZ014 <-function(){
837               list("tau_I" = rexp(1,10), "tau_P" = rexp(1,10), "beta" = rnorm(1,0,1), "delta" = rnorm(1,0,1),
838 "theta0" = rnorm(1,0,1), "effet_I"=rnorm(dim1,0,1),"effet_P"=rnorm(dim2,0,1), "inter"=inter0)
```

```
839             }
840             mod.Z014<<-jags(inits=init.funZ014,model.file = "modelZ014_code.txt",data =
841     list("visit","ab_P","dim1","dim2"),parameters.to.save =
842     c("mu","effet_I","effet_P","tau_I","tau_P","delta","beta","theta0","loglik"),n.chains = 1,
843     n.iter=1000000, n.burnin = 250000, n.thin = 250)
844             mod.Z014.mcmc<-as.mcmc(mod.Z014)
845             mZ014<-mod.Z014$BUGSoutput$sims.list
846             mZ014.deviance<-mZ014$deviance
847             mZ014.loglik<-mZ014$loglik
848             dimSEM<-dim(mZ014.loglik)[1]
849             list.mZ014<-sapply(1:dimSEM,function(x) matrix(mZ014.loglik[x,,],nrow=dim1*dim2))
850             list.tmZ014<-(t(list.mZ014))
851             mZ014.loo<-loo(list.tmZ014)
852             mZ014.loo
853             loo_file<-paste(dossier, "/", site, "_Z014_loo.txt", sep="")
854             write_values("mZ014", app=T, loo_file)
855             mZ014_loo_pointwise<-mZ014.loo$pointwise
856             mZ014_loo_pareto_k<-mZ014.loo$pareto_k
857             mZ014.loo$pareto_k<-NULL
858             mZ014.loo$pointwise<-NULL
859             write_values(as.matrix(mZ014.loo), app=T, loo_file)
860             save.image(paste(dossier, "/", site, "_Z014.RData", sep=""))
861     }
862     ### MODEL Z013
863     mZ013<-function(){
864             init.funZ013 <-function(){
```

```
865                 list("tau_I" = rexp(1,10), "tau_P" = rexp(1,10), "beta" = rnorm(1,0,1), "gamma" =
866     rnorm(1,0,1), "theta0" = rnorm(1,0,1), "effet_I"=rnorm(dim1,0,1),"effet_P"=rnorm(dim2,0,1),
867     "inter"=inter0)
868                 }
869                 mod.Z013<<-jags(inits=init.funZ013,model.file = "modelZ013_code.txt",data =
870     list("visit","ab_I","dim1","dim2"),parameters.to.save =
871     c("mu","effet_I","effet_P","tau_I","tau_P","gamma","beta","theta0","loglik"),n.chains = 1,
872     n.iter=1000000, n.burnin = 250000, n.thin = 250)
873                 mod.Z013.mcmc<-as.mcmc(mod.Z013)
874                 mZ013<-mod.Z013$BUGSoutput$sims.list
875                 mZ013.deviance<-mZ013$deviance
876                 mZ013.loglik<-mZ013$loglik
877                 dimSEM<-dim(mZ013.loglik)[1]
878                 list.mZ013<-sapply(1:dimSEM,function(x) matrix(mZ013.loglik[x,,],nrow=dim1*dim2))
879                 list.tmZ013<-(t(list.mZ013))
880                 mZ013.loo<-loo(list.tmZ013)
881                 mZ013.loo
882                 loo_file<-paste(dossier, "/", site, "_Z013_loo.txt", sep="")
883                 write_values("mZ013", app=T, loo_file)
884                 mZ013_loo_pointwise<-mZ013.loo$pointwise
885                 mZ013_loo_pareto_k<-mZ013.loo$pareto_k
886                 mZ013.loo$pareto_k<-NULL
887                 mZ013.loo$pointwise<-NULL
888                 write_values(as.matrix(mZ013.loo), app=T, loo_file)
889                 save.image(paste(dossier, "/", site, "_Z013.RData", sep=""))
890     }
```

```
### MODEL Z012
mZ012<-function(){
        init.funZ012 <-function(){
          list("tau_I" = rexp(1,10), "tau_P" = rexp(1,10), "beta" = rnorm(1,0,1), "theta0" =
rnorm(1,0,1), "epsilon" = rnorm(1,0,1), "effet_I"=rnorm(dim1,0,1),"effet_P"=rnorm(dim2,0,1),
"inter"=inter0)
        }
        mod.Z012<<-jags(inits=init.funZ012,model.file = "modelZ012_code.txt",data =
list("cooc","visit","dim1","dim2"),parameters.to.save =
c("mu","effet_I","effet_P","tau_I","tau_P","beta","theta0","epsilon","loglik"),n.chains = 1,
n.iter=1000000, n.burnin = 250000, n.thin = 250)
        mod.Z012.mcmc<-as.mcmc(mod.Z012)
        mZ012<-mod.Z012$BUGSoutput$sims.list
        mZ012.deviance<-mZ012$deviance
        mZ012.loglik<-mZ012$loglik
        dimSEM<-dim(mZ012.loglik)[1]
        list.mZ012<-sapply(1:dimSEM,function(x) matrix(mZ012.loglik[x,,],nrow=dim1*dim2))
        list.tmZ012<-(t(list.mZ012))
        mZ012.loo<-loo(list.tmZ012)
        mZ012.loo
        loo_file<-paste(dossier, "/", site, "_Z012_loo.txt", sep="")
        write_values("mZ012", app=T, loo_file)
        mZ012_loo_pointwise<-mZ012.loo$pointwise
        mZ012_loo_pareto_k<-mZ012.loo$pareto_k
        mZ012.loo$pareto_k<-NULL
        mZ012.loo$pointwise<-NULL
```

```
917             write_values(as.matrix(mZ012.loo), app=T, loo_file)
918             save.image(paste(dossier, "/", site, "_Z012.RData", sep=""))
919     }
920     ### MODEL Z011
921     mZ011<-function(){
922             init.funZ011 <-function(){
923               list("tau_I" = rexp(1,10), "tau_P" = rexp(1,10), "alpha" = 0.1,"beta" = rnorm(1,0,1), "theta0"
924     = rnorm(1,0,1), "effet_I"=rnorm(dim1,0,1),"effet_P"=rnorm(dim2,0,1), "inter"=inter0)
925             }
926             mod.Z011<<-jags(inits=init.funZ011,model.file = "modelZ011_code.txt",data =
927     list("cooc","visit","dim1","dim2"),parameters.to.save =
928     c("mu","effet_I","effet_P","tau_I","tau_P","alpha","beta","theta0","loglik"),n.chains = 1,
929     n.iter=1000000, n.burnin = 250000, n.thin = 250)
930             mod.Z011.mcmc<-as.mcmc(mod.Z011)
931             mZ011<-mod.Z011$BUGSoutput$sims.list
932             mZ011.deviance<-mZ011$deviance
933             mZ011.loglik<-mZ011$loglik
934             dimSEM<-dim(mZ011.loglik)[1]
935             list.mZ011<-sapply(1:dimSEM,function(x) matrix(mZ011.loglik[x,,],nrow=dim1*dim2))
936             list.tmZ011<-(t(list.mZ011))
937             mZ011.loo<-loo(list.tmZ011)
938             mZ011.loo
939             loo_file<-paste(dossier, "/", site, "_Z011_loo.txt", sep="")
940             write_values("mZ011", app=T, loo_file)
941             mZ011_loo_pointwise<-mZ011.loo$pointwise
942             mZ011_loo_pareto_k<-mZ011.loo$pareto_k
```

```
943             mZ011.loo$pareto_k<-NULL
944             mZ011.loo$pointwise<-NULL
945             write_values(as.matrix(mZ011.loo), app=T, loo_file)
946             save.image(paste(dossier, "/", site, "_Z011.RData", sep=""))
947     }
948     ### MODEL Z010
949     mZ010<-function(){
950             init.funZ010 <-function(){
951               list("tau_I" = rexp(1,10), "tau_P" = rexp(1,10), "beta" = rnorm(1,0,1), "gamma" =
952     rnorm(1,0,1), "delta" = rnorm(1,0,1), "theta0" = rnorm(1,0,1),
953     "effet_I"=rnorm(dim1,0,1),"effet_P"=rnorm(dim2,0,1), "inter"=inter0)
954             }
955             mod.Z010<<-jags(inits=init.funZ010,model.file = "modelZ010_code.txt",data =
956     list("visit","ab_I","ab_P","dim1","dim2"),parameters.to.save =
957     c("mu","effet_I","effet_P","tau_I","tau_P","gamma","delta","beta","theta0","loglik"),n.chains = 1,
958     n.iter=1000000, n.burnin = 250000, n.thin = 250)
959             mod.Z010.mcmc<-as.mcmc(mod.Z010)
960             mZ010<-mod.Z010$BUGSoutput$sims.list
961             mZ010.deviance<-mZ010$deviance
962             mZ010.loglik<-mZ010$loglik
963             dimSEM<-dim(mZ010.loglik)[1]
964             list.mZ010<-sapply(1:dimSEM,function(x) matrix(mZ010.loglik[x,,],nrow=dim1*dim2))
965             list.tmZ010<-(t(list.mZ010))
966             mZ010.loo<-loo(list.tmZ010)
967             mZ010.loo
968             loo_file<-paste(dossier, "/", site, "_Z010_loo.txt", sep="")
```

```
969             write_values("mZ010", app=T, loo_file)
970             mZ010_loo_pointwise<-mZ010.loo$pointwise
971             mZ010_loo_pareto_k<-mZ010.loo$pareto_k
972             mZ010.loo$pareto_k<-NULL
973             mZ010.loo$pointwise<-NULL
974             write_values(as.matrix(mZ010.loo), app=T, loo_file)
975             save.image(paste(dossier, "/", site, "_Z010.RData", sep=""))
976     }
977     ### MODEL Z09
978     mZ09<-function(){
979             init.funZ09 <-function(){
980               list("tau_I" = rexp(1,10), "tau_P" = rexp(1,10), "beta" = rnorm(1,0,1), "delta" = rnorm(1,0,1),
981     "theta0" = rnorm(1,0,1), "epsilon" = rnorm(1,0,1),
982     "effet_I"=rnorm(dim1,0,1),"effet_P"=rnorm(dim2,0,1), "inter"=inter0)
983             }
984             mod.Z09<<-jags(inits=init.funZ09,model.file = "modelZ09_code.txt",data =
985     list("cooc","visit","ab_P","dim1","dim2"),parameters.to.save =
986     c("mu","effet_I","effet_P","tau_I","tau_P","delta","beta","theta0","epsilon","loglik"),n.chains = 1,
987     n.iter=1000000, n.burnin = 250000, n.thin = 250)
988             mod.Z09.mcmc<-as.mcmc(mod.Z09)
989             mZ09<-mod.Z09$BUGSoutput$sims.list
990             mZ09.deviance<-mZ09$deviance
991             mZ09.loglik<-mZ09$loglik
992             dimSEM<-dim(mZ09.loglik)[1]
993             list.mZ09<-sapply(1:dimSEM,function(x) matrix(mZ09.loglik[x,,],nrow=dim1*dim2))
994             list.tmZ09<-(t(list.mZ09))
```

```
995             mZ09.loo<-loo(list.tmZ09)
996             mZ09.loo
997             loo_file<-paste(dossier, "/", site, "_Z09_loo.txt", sep="")
998             write_values("mZ09", app=T, loo_file)
999             mZ09_loo_pointwise<-mZ09.loo$pointwise
1000            mZ09_loo_pareto_k<-mZ09.loo$pareto_k
1001            mZ09.loo$pareto_k<-NULL
1002            mZ09.loo$pointwise<-NULL
1003            write_values(as.matrix(mZ09.loo), app=T, loo_file)
1004            save.image(paste(dossier, "/", site, "_Z09.RData", sep=""))
1005    }
1006    ### MODEL Z08
1007    mZ08<-function(){
1008            init.funZ08 <-function(){
1009              list("tau_I" = rexp(1,10), "tau_P" = rexp(1,10), "beta" = rnorm(1,0,1), "gamma" =
1010    rnorm(1,0,1), "theta0" = rnorm(1,0,1), "epsilon" = rnorm(1,0,1),
1011    "effet_I"=rnorm(dim1,0,1),"effet_P"=rnorm(dim2,0,1), "inter"=inter0)
1012            }
1013            mod.Z08<<-jags(inits=init.funZ08,model.file = "modelZ08_code.txt",data =
1014    list("cooc","visit","ab_I","dim1","dim2"),parameters.to.save =
1015    c("mu","effet_I","effet_P","tau_I","tau_P","gamma","beta","theta0","epsilon","loglik"),n.chains = 1,
1016    n.iter=1000000, n.burnin = 250000, n.thin = 250)
1017            mod.Z08.mcmc<-as.mcmc(mod.Z08)
1018            mZ08<-mod.Z08$BUGSoutput$sims.list
1019            mZ08.deviance<-mZ08$deviance
1020            mZ08.loglik<-mZ08$loglik
```

```
1021            dimSEM<-dim(mZ08.loglik)[1]
1022            list.mZ08<-sapply(1:dimSEM,function(x) matrix(mZ08.loglik[x,,],nrow=dim1*dim2))
1023            list.tmZ08<-(t(list.mZ08))
1024            mZ08.loo<-loo(list.tmZ08)
1025            mZ08.loo
1026            loo_file<-paste(dossier, "/", site, "_Z08_loo.txt", sep="")
1027            write_values("mZ08", app=T, loo_file)
1028            mZ08_loo_pointwise<-mZ08.loo$pointwise
1029            mZ08_loo_pareto_k<-mZ08.loo$pareto_k
1030            mZ08.loo$pareto_k<-NULL
1031            mZ08.loo$pointwise<-NULL
1032            write_values(as.matrix(mZ08.loo), app=T, loo_file)
1033            save.image(paste(dossier, "/", site, "_Z08.RData", sep=""))
1034    }
1035    ### MODEL Z07
1036    mZ07<-function(){
1037            init.funZ07 <-function(){
1038              list("tau_I" = rexp(1,10), "tau_P" = rexp(1,10), "alpha" = 0.1,"beta" = rnorm(1,0,1), "delta" =
1039    rnorm(1,0,1), "theta0" = rnorm(1,0,1), "effet_I"=rnorm(dim1,0,1),"effet_P"=rnorm(dim2,0,1),
1040    "inter"=inter0)
1041            }
1042            mod.Z07<<-jags(inits=init.funZ07,model.file = "modelZ07_code.txt",data =
1043    list("cooc","visit","ab_P","dim1","dim2"),parameters.to.save =
1044    c("mu","effet_I","effet_P","tau_I","tau_P","alpha","delta","beta","theta0","loglik"),n.chains = 1,
1045    n.iter=1000000, n.burnin = 250000, n.thin = 250)
1046            mod.Z07.mcmc<-as.mcmc(mod.Z07)
```

```
1047            mZ07<-mod.Z07$BUGSoutput$sims.list
1048            mZ07.deviance<-mZ07$deviance
1049            mZ07.loglik<-mZ07$loglik
1050            dimSEM<-dim(mZ07.loglik)[1]
1051            list.mZ07<-sapply(1:dimSEM,function(x) matrix(mZ07.loglik[x,,],nrow=dim1*dim2))
1052            list.tmZ07<-(t(list.mZ07))
1053            mZ07.loo<-loo(list.tmZ07)
1054            mZ07.loo
1055            loo_file<-paste(dossier, "/", site, "_Z07_loo.txt", sep="")
1056            write_values("mZ07", app=T, loo_file)
1057            mZ07_loo_pointwise<-mZ07.loo$pointwise
1058            mZ07_loo_pareto_k<-mZ07.loo$pareto_k
1059            mZ07.loo$pareto_k<-NULL
1060            mZ07.loo$pointwise<-NULL
1061            write_values(as.matrix(mZ07.loo), app=T, loo_file)
1062            save.image(paste(dossier, "/", site, "_Z07.RData", sep=""))
1063    }
1064    ### MODEL Z06
1065    mZ06<-function(){
1066            init.funZ06 <-function(){
1067              list("tau_I" = rexp(1,10), "tau_P" = rexp(1,10), "alpha" = 0.1,"beta" = rnorm(1,0,1), "gamma"
1068    = rnorm(1,0,1), "theta0" = rnorm(1,0,1), "effet_I"=rnorm(dim1,0,1),"effet_P"=rnorm(dim2,0,1),
1069    "inter"=inter0)
1070            }
1071            mod.Z06<<-jags(inits=init.funZ06,model.file = "modelZ06_code.txt",data =
1072    list("cooc","visit","ab_I","dim1","dim2"),parameters.to.save =
```

```
c("mu","effet_I","effet_P","tau_I","tau_P","alpha","gamma","beta","theta0","loglik"),n.chains = 1,
n.iter=1000000, n.burnin = 250000, n.thin = 250)
        mod.Z06.mcmc<-as.mcmc(mod.Z06)
        mZ06<-mod.Z06$BUGSoutput$sims.list
        mZ06.deviance<-mZ06$deviance
        mZ06.loglik<-mZ06$loglik
        dimSEM<-dim(mZ06.loglik)[1]
        list.mZ06<-sapply(1:dimSEM,function(x) matrix(mZ06.loglik[x,,],nrow=dim1*dim2))
        list.tmZ06<-(t(list.mZ06))
        mZ06.loo<-loo(list.tmZ06)
        mZ06.loo
        loo_file<-paste(dossier, "/", site, "_Z06_loo.txt", sep="")
        write_values("mZ06", app=T, loo_file)
        mZ06_loo_pointwise<-mZ06.loo$pointwise
        mZ06_loo_pareto_k<-mZ06.loo$pareto_k
        mZ06.loo$pareto_k<-NULL
        mZ06.loo$pointwise<-NULL
        write_values(as.matrix(mZ06.loo), app=T, loo_file)
        save.image(paste(dossier, "/", site, "_Z06.RData", sep=""))
}
### MODEL Z05
mZ05<-function(){
        init.funZ05 <-function(){
          list("tau_I" = rexp(1,10), "tau_P" = rexp(1,10), "alpha" = 0.1,"beta" = rnorm(1,0,1), "theta0"
= rnorm(1,0,1), "epsilon" = rnorm(1,0,1), "effet_I"=rnorm(dim1,0,1),"effet_P"=rnorm(dim2,0,1),
"inter"=inter0)
```

```
1099            }
1100            mod.Z05<<-jags(inits=init.funZ05,model.file = "modelZ05_code.txt",data =
1101    list("cooc","visit","dim1","dim2"),parameters.to.save =
1102    c("mu","effet_I","effet_P","tau_I","tau_P","alpha","beta","theta0","epsilon","loglik"),n.chains = 1,
1103    n.iter=1000000, n.burnin = 250000, n.thin = 250)
1104            mod.Z05.mcmc<-as.mcmc(mod.Z05)
1105            mZ05<-mod.Z05$BUGSoutput$sims.list
1106            mZ05.deviance<-mZ05$deviance
1107            mZ05.loglik<-mZ05$loglik
1108            dimSEM<-dim(mZ05.loglik)[1]
1109            list.mZ05<-sapply(1:dimSEM,function(x) matrix(mZ05.loglik[x,,],nrow=dim1*dim2))
1110            list.tmZ05<-(t(list.mZ05))
1111            mZ05.loo<-loo(list.tmZ05)
1112            mZ05.loo
1113            loo_file<-paste(dossier, "/", site, "_Z05_loo.txt", sep="")
1114            write_values("mZ05", app=T, loo_file)
1115            mZ05_loo_pointwise<-mZ05.loo$pointwise
1116            mZ05_loo_pareto_k<-mZ05.loo$pareto_k
1117            mZ05.loo$pareto_k<-NULL
1118            mZ05.loo$pointwise<-NULL
1119            write_values(as.matrix(mZ05.loo), app=T, loo_file)
1120            save.image(paste(dossier, "/", site, "_Z05.RData", sep=""))
1121    }
1122    ### MODEL Z04
1123    mZ04<-function(){
1124            init.funZ04 <-function(){
```

```
1125                 list("tau_I" = rexp(1,10), "tau_P" = rexp(1,10), "beta" = rnorm(1,0,1), "gamma" =
1126    rnorm(1,0,1), "delta" = rnorm(1,0,1), "theta0" = rnorm(1,0,1), "epsilon" = rnorm(1,0,1),
1127    "effet_I"=rnorm(dim1,0,1),"effet_P"=rnorm(dim2,0,1), "inter"=inter0)
1128             }
1129             mod.Z04<<-jags(inits=init.funZ04,model.file = "modelZ04_code.txt",data =
1130    list("cooc","visit","ab_I","ab_P","dim1","dim2"),parameters.to.save =
1131    c("mu","effet_I","effet_P","tau_I","tau_P","gamma","delta","beta","theta0","epsilon","loglik"),n.chai
1132    ns = 1, n.iter=1000000, n.burnin = 250000, n.thin = 250)
1133             mod.Z04.mcmc<-as.mcmc(mod.Z04)
1134             mZ04<-mod.Z04$BUGSoutput$sims.list
1135             mZ04.deviance<-mZ04$deviance
1136             mZ04.loglik<-mZ04$loglik
1137             dimSEM<-dim(mZ04.loglik)[1]
1138             list.mZ04<-sapply(1:dimSEM,function(x) matrix(mZ04.loglik[x,,],nrow=dim1*dim2))
1139             list.tmZ04<-(t(list.mZ04))
1140             mZ04.loo<-loo(list.tmZ04)
1141             mZ04.loo
1142             loo_file<-paste(dossier, "/", site, "_Z04_loo.txt", sep="")
1143             write_values("mZ04", app=T, loo_file)
1144             mZ04_loo_pointwise<-mZ04.loo$pointwise
1145             mZ04_loo_pareto_k<-mZ04.loo$pareto_k
1146             mZ04.loo$pareto_k<-NULL
1147             mZ04.loo$pointwise<-NULL
1148             write_values(as.matrix(mZ04.loo), app=T, loo_file)
1149             save.image(paste(dossier, "/", site, "_Z04.RData", sep=""))
1150    }
```

```
### MODEL Z03
mZ03<-function(){
        init.funZ03 <-function(){
          list("tau_I" = rexp(1,10), "tau_P" = rexp(1,10), "alpha" = 0.1,"beta" = rnorm(1,0,1), "gamma"
= rnorm(1,0,1), "theta0" = rnorm(1,0,1), "epsilon" = rnorm(1,0,1),
"effet_I"=rnorm(dim1,0,1),"effet_P"=rnorm(dim2,0,1), "inter"=inter0)
        }
        mod.Z03<<-jags(inits=init.funZ03,model.file = "modelZ03_code.txt",data =
list("cooc","visit","ab_I","dim1","dim2"),parameters.to.save =
c("mu","effet_I","effet_P","tau_I","tau_P","alpha","gamma","beta","theta0","epsilon","loglik"),n.cha
ins = 1, n.iter=1000000, n.burnin = 250000, n.thin = 250)
        mod.Z03.mcmc<-as.mcmc(mod.Z03)
        mZ03<-mod.Z03$BUGSoutput$sims.list
        mZ03.deviance<-mZ03$deviance
        mZ03.loglik<-mZ03$loglik
        dimSEM<-dim(mZ03.loglik)[1]
        list.mZ03<-sapply(1:dimSEM,function(x) matrix(mZ03.loglik[x,,],nrow=dim1*dim2))
        list.tmZ03<-(t(list.mZ03))
        mZ03.loo<-loo(list.tmZ03)
        mZ03.loo
        loo_file<-paste(dossier, "/", site, "_Z03_loo.txt", sep="")
        write_values("mZ03", app=T, loo_file)
        mZ03_loo_pointwise<-mZ03.loo$pointwise
        mZ03_loo_pareto_k<-mZ03.loo$pareto_k
        mZ03.loo$pareto_k<-NULL
        mZ03.loo$pointwise<-NULL
```

```
1177            write_values(as.matrix(mZ03.loo), app=T, loo_file)
1178            save.image(paste(dossier, "/", site, "_Z03.RData", sep=""))
1179    }
1180    ### MODEL Z02
1181    mZ02<-function(){
1182            init.funZ02 <-function(){
1183              list("tau_I" = rexp(1,10), "tau_P" = rexp(1,10), "alpha" = 0.1, "beta" = rnorm(1,0,1), "delta" =
1184    rnorm(1,0,1), "theta0" = rnorm(1,0,1), "epsilon" = rnorm(1,0,1),
1185    "effet_I"=rnorm(dim1,0,1),"effet_P"=rnorm(dim2,0,1), "inter"=inter0)
1186            }
1187            mod.Z02<<-jags(inits=init.funZ02,model.file = "modelZ02_code.txt",data =
1188    list("cooc","visit","ab_P","dim1","dim2"),parameters.to.save =
1189    c("mu","effet_I","effet_P","tau_I","tau_P","alpha","delta","beta","theta0","epsilon","loglik"),n.chain
1190    s = 1, n.iter=1000000, n.burnin = 250000, n.thin = 250)
1191            mod.Z02.mcmc<-as.mcmc(mod.Z02)
1192            mZ02<-mod.Z02$BUGSoutput$sims.list
1193            mZ02.deviance<-mZ02$deviance
1194            mZ02.loglik<-mZ02$loglik
1195            dimSEM<-dim(mZ02.loglik)[1]
1196            list.mZ02<-sapply(1:dimSEM,function(x) matrix(mZ02.loglik[x,,],nrow=dim1*dim2))
1197            list.tmZ02<-(t(list.mZ02))
1198            mZ02.loo<-loo(list.tmZ02)
1199            mZ02.loo
1200            loo_file<-paste(dossier, "/", site, "_Z02_loo.txt", sep="")
1201            write_values("mZ02", app=T, loo_file)
1202            mZ02_loo_pointwise<-mZ02.loo$pointwise
```

```
1203            mZ02_loo_pareto_k<-mZ02.loo$pareto_k
1204            mZ02.loo$pareto_k<-NULL
1205            mZ02.loo$pointwise<-NULL
1206            write_values(as.matrix(mZ02.loo), app=T, loo_file)
1207            save.image(paste(dossier, "/", site, "_Z02.RData", sep=""))
1208    }
1209    ### MODEL Z01
1210    mZ01<-function(){
1211            init.funZ01 <-function(){
1212              list("tau_I" = rexp(1,10), "tau_P" = rexp(1,10), "alpha" = 0.1,"beta" = rnorm(1,0,1), "gamma"
1213    = rnorm(1,0,1), "delta" = rnorm(1,0,1), "theta0" = rnorm(1,0,1),
1214    "effet_I"=rnorm(dim1,0,1),"effet_P"=rnorm(dim2,0,1), "inter"=inter0)
1215            }
1216            mod.Z01<<-jags(inits=init.funZ01,model.file = "modelZ01_code.txt",data =
1217    list("cooc","visit","ab_I","ab_P", "dim1", "dim2"),parameters.to.save =
1218    c("mu","effet_I","effet_P","tau_I","tau_P","alpha","gamma","delta","beta","theta0","loglik"),n.chain
1219    s = 1, n.iter=1000000, n.burnin = 250000, n.thin = 250)
1220            mod.Z01.mcmc<-as.mcmc(mod.Z01)
1221            mZ01<-mod.Z01$BUGSoutput$sims.list
1222            mZ01.deviance<-mZ01$deviance
1223            mZ01.loglik<-mZ01$loglik
1224            dimSEM<-dim(mZ01.loglik)[1]
1225            list.mZ01<-sapply(1:dimSEM,function(x) matrix(mZ01.loglik[x,,],nrow=dim1*dim2))
1226            list.tmZ01<-(t(list.mZ01))
1227            mZ01.loo<-loo(list.tmZ01)
1228            mZ01.loo
```

```
1229            loo_file<-paste(dossier, "/", site, "_Z01_loo.txt", sep="")
1230            write_values("mZ01", app=T, loo_file)
1231            mZ01_loo_pointwise<-mZ01.loo$pointwise
1232            mZ01_loo_pareto_k<-mZ01.loo$pareto_k
1233            mZ01.loo$pareto_k<-NULL
1234            mZ01.loo$pointwise<-NULL
1235            write_values(as.matrix(mZ01.loo), app=T, loo_file)
1236            save.image(paste(dossier, "/", site, "_Z01.RData", sep=""))
1237    }
1238    ### MODEL Z00
1239    mZ00<-function(){
1240            init.funZ00 <-function(){
1241              list("tau_I" = rexp(1,10), "tau_P" = rexp(1,10), "alpha" = 0.1,"beta" = rnorm(1,0,1), "gamma"
1242    = rnorm(1,0,1), "delta" = rnorm(1,0,1), "theta0" = rnorm(1,0,1), "epsilon" = rnorm(1,0,1),
1243    "effet_I"=rnorm(dim1,0,1),"effet_P"=rnorm(dim2,0,1), "inter"=inter0)
1244            }
1245            mod.Z00<<-jags(inits=init.funZ00,model.file = "modelZ00_code.txt",data =
1246    list("cooc","visit","ab_I","ab_P","dim1","dim2"),parameters.to.save =
1247    c("mu","effet_I","effet_P","tau_I","tau_P","alpha","gamma","delta","beta","theta0","epsilon","loglik
1248    "),n.chains = 1, n.iter=1000000, n.burnin = 250000, n.thin = 250)
1249            mod.Z00.mcmc<-as.mcmc(mod.Z00)
1250            mZ00<-mod.Z00$BUGSoutput$sims.list
1251            mZ00.deviance<-mZ00$deviance
1252            mZ00.loglik<-mZ00$loglik
1253            dimSEM<-dim(mZ00.loglik)[1]
1254            list.mZ00<-sapply(1:dimSEM,function(x) matrix(mZ00.loglik[x,,],nrow=dim1*dim2))
```

```
1255            list.tmZ00<-(t(list.mZ00))
1256            mZ00.loo<-loo(list.tmZ00)
1257            mZ00.loo
1258            loo_file<-paste(dossier, "/", site, "_Z00_loo.txt", sep="")
1259            write_values("mZ00", app=T, loo_file)
1260            mZ00_loo_pointwise<-mZ00.loo$pointwise
1261            mZ00_loo_pareto_k<-mZ00.loo$pareto_k
1262            mZ00.loo$pareto_k<-NULL
1263            mZ00.loo$pointwise<-NULL
1264            write_values(as.matrix(mZ00.loo), app=T, loo_file)
1265            save.image(paste(dossier, "/", site, "_Z00.RData", sep=""))
1266    }
1267    ###### end model functions
1268    print("JOB DONE")
1269    ######################################################
1270    ###     Network information (do not change)    ###
1271    ######################################################
1272    ##############################BLOCK 3 – MODEL EXECUTION ########################
1273    #launch_modele<-function(){
1274            ntw<-read.table(paste(dossier, "/", site, "_ntw.txt", sep=""),
1275    sep="\t",header=T,row.names=1)
1276            dim1<-dim(ntw)[1]
1277            dim2<-dim(ntw)[2]
1278            web<-as.matrix(ntw,dim1,dim2)
1279            inter0<-dget(paste(dossier, "/", site, "_web_i.txt", sep=""))
1280            cooc<-dget(paste(dossier, "/", site, "_co.txt", sep=""))
```

```
1281            visit<-read.table(paste(dossier, "/", site, "_ntw.txt", sep=""),sep="\t",header=T)
1282            visit<-as.matrix(visit)
1283            abundanceI<-read.table(paste(dossier, "/", site, "_abI.txt", sep=""), sep="\t", header=T)
1284            ab_I <- log(abundanceI[,2])
1285            abundanceP<-read.table(paste(dossier, "/", site, "_abP.txt", sep=""), sep="\t", header=T)
1286            ab_P <- log(abundanceP[,2])
1287            if(opt$modele == "all")
1288            {
1289                    print("modele: all")
1290                    for(i in 0:15)
1291                    {
1292                            print(paste("COMPUTING MODELE ", i, "\n", sep=""))
1293                            mod<-eval(parse(text=paste("mZ0", i, sep="")))
1294                            mod()
1295
1296                    }
1297            }else{
1298                    print(paste("modele: ", opt$modele), sep="")
1299                    mod<-eval(parse(text=paste("m", opt$modele, sep="")))          #recupération de la
1300    fonction du modele
1301                    mod()
1302            }
1303    #### end model execution
1304    #launch_modele()
1305
1306    ################################PARAMETER VALUES################################
```

```
library(optparse)
option_list = list(
	make_option(c("-d", "--dir"), type="character", default=NULL, help="model directory",
metavar="character"),
	make_option(c("-s", "--site"), type="character", default=NULL, help="site name",
metavar="character"))
opt_parser = OptionParser(option_list=option_list);
opt = parse_args(opt_parser);
rdata<-list.files(opt$dir, pattern="*_Z015.RData")
load(paste(opt$dir, "/", rdata, sep="")) #chargement du RData qui contient tous les modèles pour un
site donné
print(paste("RData ", rdata, " loaded", sep=""))
for(mod in ls(pattern="mod.Z0*"))
{
	print(paste("getting values from ", mod, sep=""))
	model<-eval(parse(text=mod))
	if(is.null(model$BUGSoutput$mean$alpha)){model$BUGSoutput$mean$alpha<-NA}
	if(is.null(model$BUGSoutput$mean$beta)){model$BUGSoutput$mean$beta<-NA}
	if(is.null(model$BUGSoutput$mean$delta)){model$BUGSoutput$mean$delta<-NA}
	if(is.null(model$BUGSoutput$mean$epsilon)){model$BUGSoutput$mean$epsilon<-NA}
	if(is.null(model$BUGSoutput$mean$gamma)){model$BUGSoutput$mean$gamma<-NA}
	val<-matrix(c(model$BUGSoutput$mean$alpha, model$BUGSoutput$mean$beta,
model$BUGSoutput$mean$delta, model$BUGSoutput$mean$epsilon,
model$BUGSoutput$mean$gamma), 1, 5, dimnames=list("values", c("alpha", "beta", "delta",
"epsilon", "gamma")))
```

```
1332                write.table(val, file=paste(opt$dir, "/", opt$site, "_", mod, "_values.txt", sep=""), quote=F,
1333    sep="\t", row.names=F, col.names=T)
1334    }
1335
```

Appendix S3: Modularity and latent block model analysis

We calculated the modularity of the network using the `cluster_leading_eigen` method for modularity optimization implemented in the `igraph` package (Csardi and Nepusz 2006, Newman 2006). We then performed latent block models (LBM) using the `BM_poisson` method for quantitative network data implemented in the `blockmodels` package (Leger et al. 2015). Blocks are calculated separately for the two groups (insect and plant) based on the number of visits (*i.e.* a weighted network). The algorithm finds the best divisions of insects and plants through fitting one Poisson parameter in each block of the visit matrix, thus essentially maximizing the ICL (Integrated Completed Likelihood; Biernacki et al. 2000, Daudin et al. 2007).

```
library(bipartite)
library(vegan)
library(igraph)
library(dummies)
library(blockmodels)
library(ade4)
library(fields)

#site data (ex: Bois de Fontaret, BFs)
BFs<-read.table("ntwBFs.txt",header=T,sep="\t")
webBFs <- as.matrix(BFs)
############################ Modularity analysis, binary data ##########################
BFs.graph.bin<-graph_from_incidence_matrix(webBFs,multiple=F) #binary
BFs.bin.cle<-cluster_leading_eigen(BFs.graph.bin)
BFs.bin.cle
#get phenology overlap matrix
```

```
coBF<-dget("coBFs.txt")
########################## LBM code: LBM analysis following Poisson ###################
bmi_BFs<-BM_poisson('LBM', webBFs)
bmi_BFs$estimate()
numi_BFs<-which.max(bmi_BFs$ICL)
densi_BFs<-sum(webBFs)/(nrow(webBFs)*ncol(webBFs))
probi_BFs<-bmi_BFs$model_parameters[[numi_BFs]]$lambda
row.nb.gpi<-nrow(probi_BFs)
col.nb.gpi<-ncol(probi_BFs)
prob.rowi<-bmi_BFs$memberships[[numi_BFs]]$Z1
hh.namei<-rownames(webBFs)
mbrshp.hhi<-apply(prob.rowi,1,which.max)
ls.freq.rowi<-rowSums(webBFs)
res.hhi<-cbind.data.frame(hh.namei=hh.namei, mbrshp.hhi=mbrshp.hhi, freq.hhi=ls.freq.rowi)
res.hh.ordi<-res.hhi[order(res.hhi$freq.hhi),]
cpt=0
for(k in 1: (nrow(res.hh.ordi)-1))
{
  if (res.hh.ordi$mbrshp.hhi[k] !=res.hh.ordi$mbrshp.hhi[k+1]) cpt=cpt+1
}
nb.diff.hhi=cpt-(length(levels(as.factor(res.hh.ordi$mbrshp.hhi)))-1)
#write tables
write.table(res.hh.ordi,sep="\t",row.names=FALSE)
prob.coli<-bmi_BFs$memberships[[numi_BFs]]$Z2
sp.namei<-colnames(webBFs)
mbrshp.spi<-apply(prob.coli,1,which.max)
```

```
ls.freq.coli<-colSums(webBFs)
res.spi<-cbind.data.frame(sp.namei=sp.namei, mbrshp.spi=mbrshp.spi, freq.spi=ls.freq.coli)
res.sp.ordi<-res.spi[order(res.spi$freq.spi),]
cpt=0
for (k in 1: (nrow(res.sp.ordi)-1))
{
  if(res.sp.ordi$mbrshp.spi[k] !=res.sp.ordi$mbrshp.spi[k+1]) cpt=cpt+1
}
nb.diff.spi=cpt-(length(levels(as.factor(res.sp.ordi$mbrshp.spi)))-1)
res.sp.ord2i=res.spi[order(res.spi$mbrshp.spi),]
write.table(res.sp.ordi,sep="\t",row.names=FALSE)
write.table(probi_BFs,file="_prob_BFs",sep="\t",row.names=FALSE)

################################## Matrix organization ###############
par(mfrow=c(1,1))
webBFs2<-webBFs
webBFs[which(webBFs>1)]=1
nb.row=nrow(webBFs)
nb.col=ncol(webBFs)
nds=webBFs
nps=coBF
res.prob=read.table("_prob_BFs",sep="\t",h=TRUE)
ls.ord.col.prob=order(colSums(res.prob),decreasing=TRUE)
ls.ord.row.prob=order(rowSums(res.prob),decreasing=TRUE)
ls.ord.hhi=sapply(res.hhi$mbrshp.hhi,function(x) which (x==ls.ord.row.prob))
res.hh.ord2i=res.hhi[order(ls.ord.hhi),]
```

```
row.nb.gpi=length(levels(as.factor(res.hhi$mbrshp.hhi)))
res.hh.ord3i=NULL
for (h in ls.ord.row.prob)
{
 part=res.hh.ord2i[res.hh.ord2i$mbrshp.hhi==h,]
 part.ord=part[order(part$freq.hhi,decreasing=TRUE),]
 res.hh.ord3i=rbind.data.frame(res.hh.ord3i,part.ord)
}
ls.ord.sp=sapply(res.spi$mbrshp.spi,function(x) which (x==ls.ord.col.prob))
res.sp.ord2i=res.spi[order(ls.ord.sp),]
col.nb.gb=length(levels(as.factor(res.spi$mbrshp.spi)))
res.sp.ord3i=NULL
for (h in ls.ord.col.prob)
{
 part=res.sp.ord2i[res.sp.ord2i$mbrshp.spi==h,]
 part.ord=part[order(part$freq.spi,decreasing=TRUE),]
 res.sp.ord3i=rbind.data.frame(res.sp.ord3i,part.ord)
}
nds=nds[as.character(res.hh.ord3i$hh.namei),as.character(res.sp.ord3i$sp.namei)]
nps=nps[as.character(res.hh.ord3i$hh.namei),as.character(res.sp.ord3i$sp.namei)]
webBFs2=webBFs2[as.character(res.hh.ord3i$hh.namei),as.character(res.sp.ord3i$sp.namei)]

######## Plot matrix with heatcolours and the number of visits #######
visits<-matrix(webBFs2,nrow=dim(webBFs2)[1]*dim(webBFs2)[2],ncol=1)
visits<-visits[which(visits>0)] #without the zeros
coord.function<-function(x,nI,nP){
```

```
1440      c(((x-1)%%nI)+1,((x-1)%/%nI)+1)
1441    }
1442    func.plot.matrix<-function(x,y){
1443      indices<-which(x==1)
1444      min<-min(y)
1445      max<-max(y)
1446      yLabels<-rownames(x)
1447      xLabels<-colnames(x)
1448      title<-c("Bois de Fontaret")
1449      if(is.null(xLabels)){
1450        xLabels<-c(1:ncol(x))
1451      }
1452      if(is.null(yLabels)){
1453        yLabels<-c(1:nrow(x))
1454      }
1455      reverse<-nrow(x):1
1456      yLabels<-yLabels[reverse]
1457      y<-y[reverse,]
1458      image.plot(1:length(xLabels),1:length(yLabels),t(y),col=c("white",heat.colors(12)[12:1]), xlab="",
1459    ylab="",axes=FALSE,zlim=c(min,max))
1460      if(!is.null(title)){
1461        title(ylab="Insects", line=8, cex.lab=1)
1462        title(xlab="Plants", line=6, cex.lab=1.2)
1463        title("Bois de Fontaret")
1464      }
1465      axis(BELOW<-1,at=1:length(xLabels),labels=as.factor(as.character(xLabels)),las =2, cex.axis=0.6)
```

```
1466    axis(LEFT<-2,at=1:length(yLabels), labels=as.factor(as.character(yLabels)),las= 2,cex.axis=0.6)
1467    axis(BELOW<-1,at=1:length(xLabels),labels=rep("",length(xLabels)),las =2,cex.axis=0.6)
1468    axis(LEFT<-2,at=1:length(yLabels),labels=rep("",length(yLabels)),las=2,cex.axis<-0.6)
1469    coo<-t(rbind(sapply(indices,function(xx) coord.function(xx,nrow(x),ncol(x)))))
1470    text(coo[,2],nrow(webBFs)+1-coo[,1],labels=visits, cex=0.6)
1471  }
1472  func.plot.matrix(nds,nps)
1473  ####### Black lines to delimit blocks in the plot ######
1474  if (row.nb.gpi>1)
1475  {
1476    ls.class=as.numeric(as.data.frame(table(res.hh.ord2i$mbrshp.hhi))[ls.ord.row.prob,2])
1477    ls.cum=sum(ls.class)-cumsum(ls.class)
1478    abline(h=ls.cum+0.5,col="grey20", lwd=3)
1479  }
1480  if (col.nb.gpi>1)
1481  {
1482    ls.class=as.numeric(as.data.frame(table(res.sp.ord2i$mbrshp.spi))[ls.ord.col.prob,2])
1483    ls.cum=cumsum(ls.class)
1484    abline(v=ls.cum+0.5,col="grey20", lwd=3)
1485  }
```

Figures and Tables

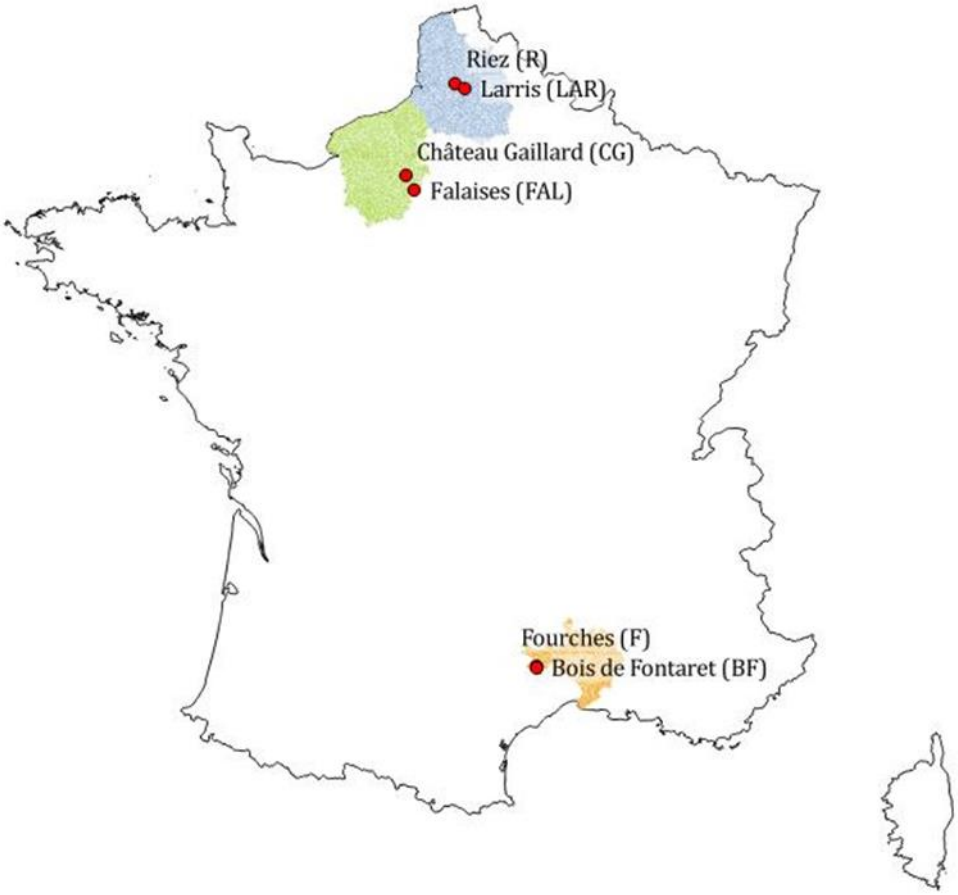

Figure S1. Site location in France: in blue the French départements Pas-de-Calais and Somme (Hauts-de-France region), in green the départements Eure and Seine Maritime (Normandie region), in orange the department Gard (Occitanie region). The six sites correspond to the red dots.

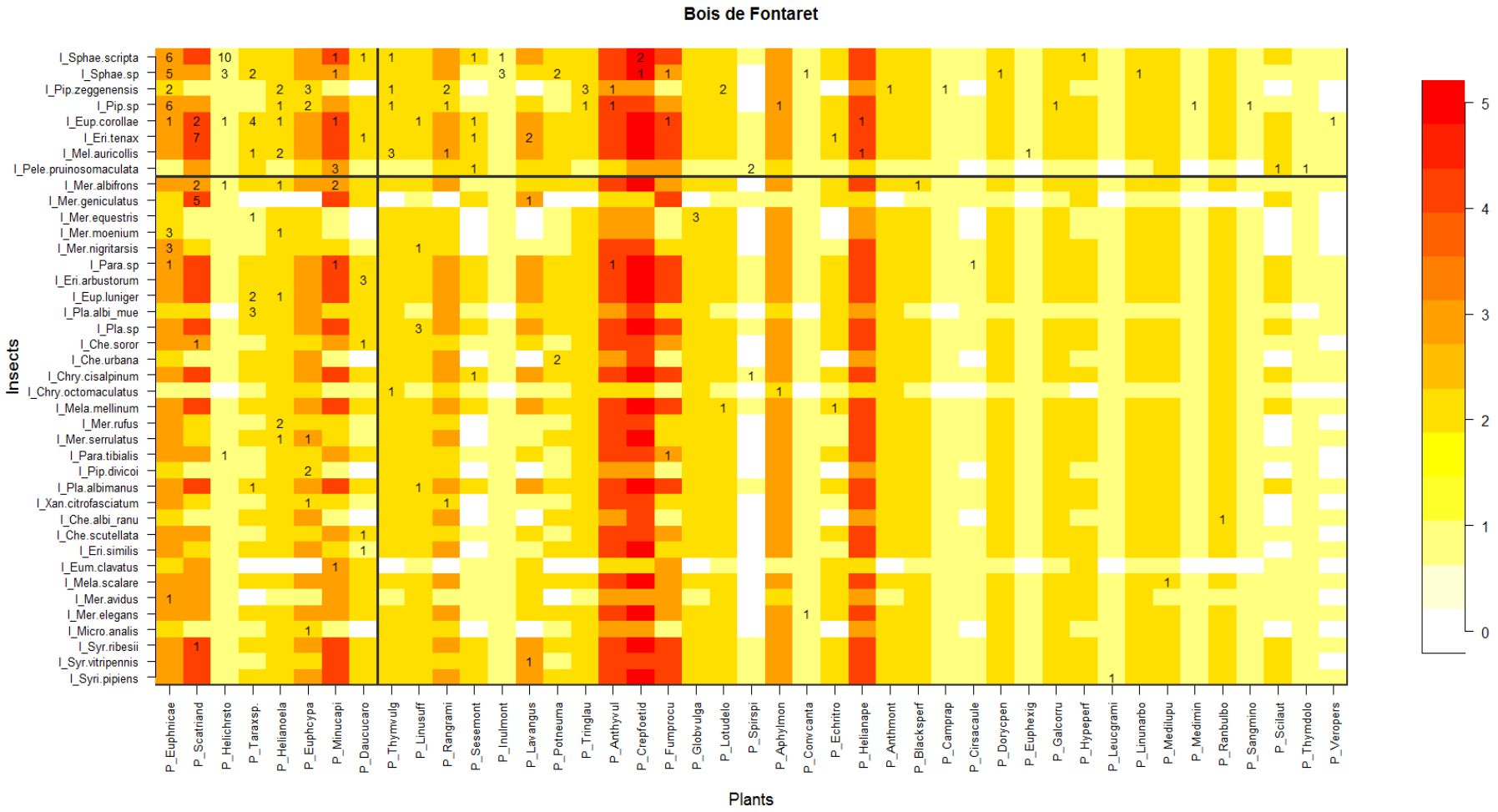

Figure S2. Block clustering provided by LBM in the site of Bois de Fontaret (BF, Occitanie), overlaid on a heatmap of species phenology overlap. Insect species are displayed in rows and plant species in columns, following their degree (number of partners). The blocks of insects and the blocks of plants are separated by solid black lines. Colours correspond to the number of months that are shared by each pair of plant and insect species (PO, phenology overlap), with higher PO corresponding to darker colours. Numbers are the number of visits observed in the field for a given plant-insect pair.

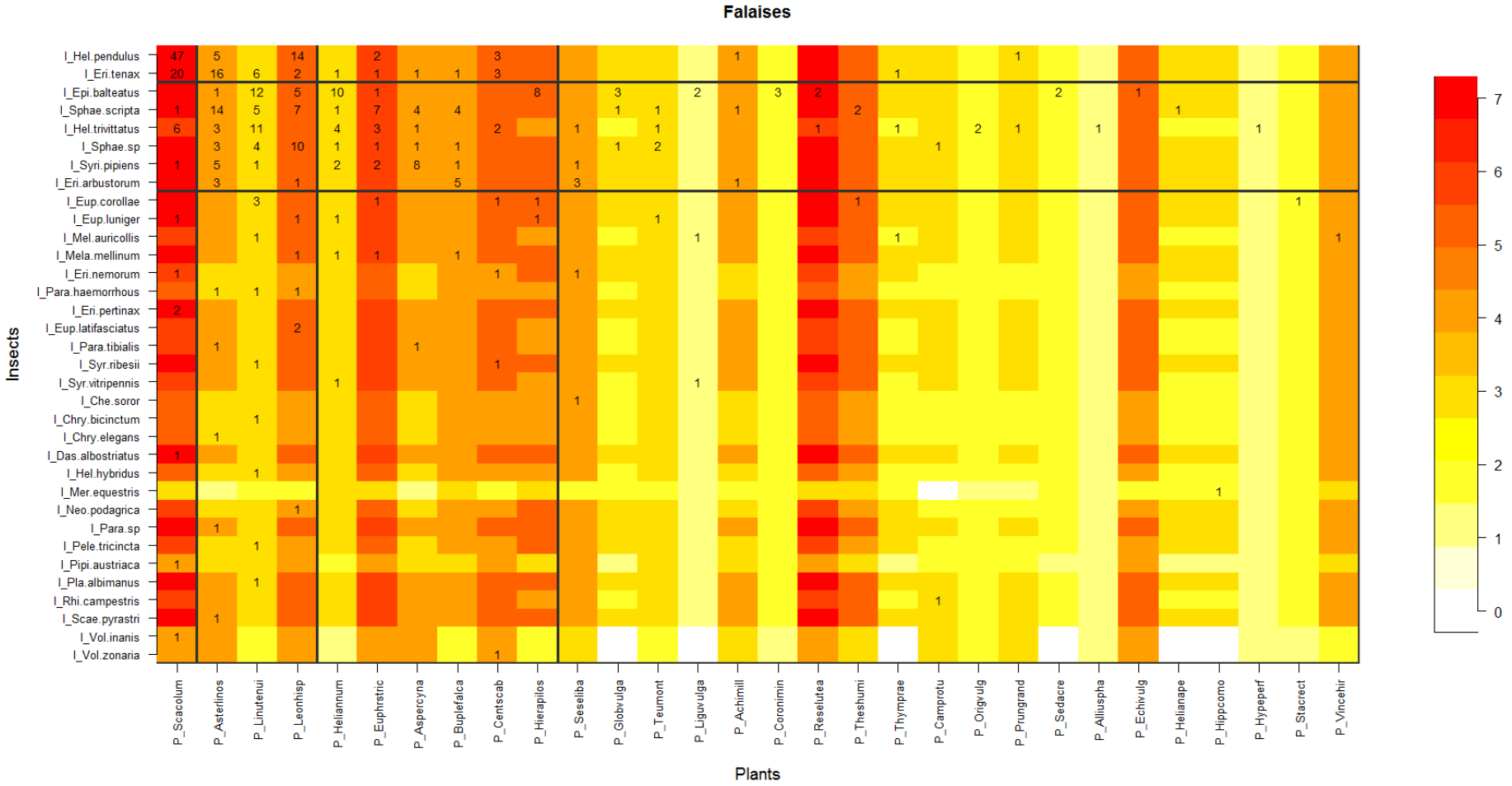

Figure S3. Block clustering provided by LBM in the site of Falaises (FAL, Normandie), overlaid on a heatmap of species phenology overlap. Insect species are displayed in rows and plant species in columns, following their degree (number of partners). The blocks of insects and the blocks of plants are separated by solid black lines. Colours correspond to the number of months that are shared by each pair of plant and insect species (PO, phenology overlap), with higher PO corresponding to darker colours. Numbers are the number of visits observed in the field for a given plant-insect pair.

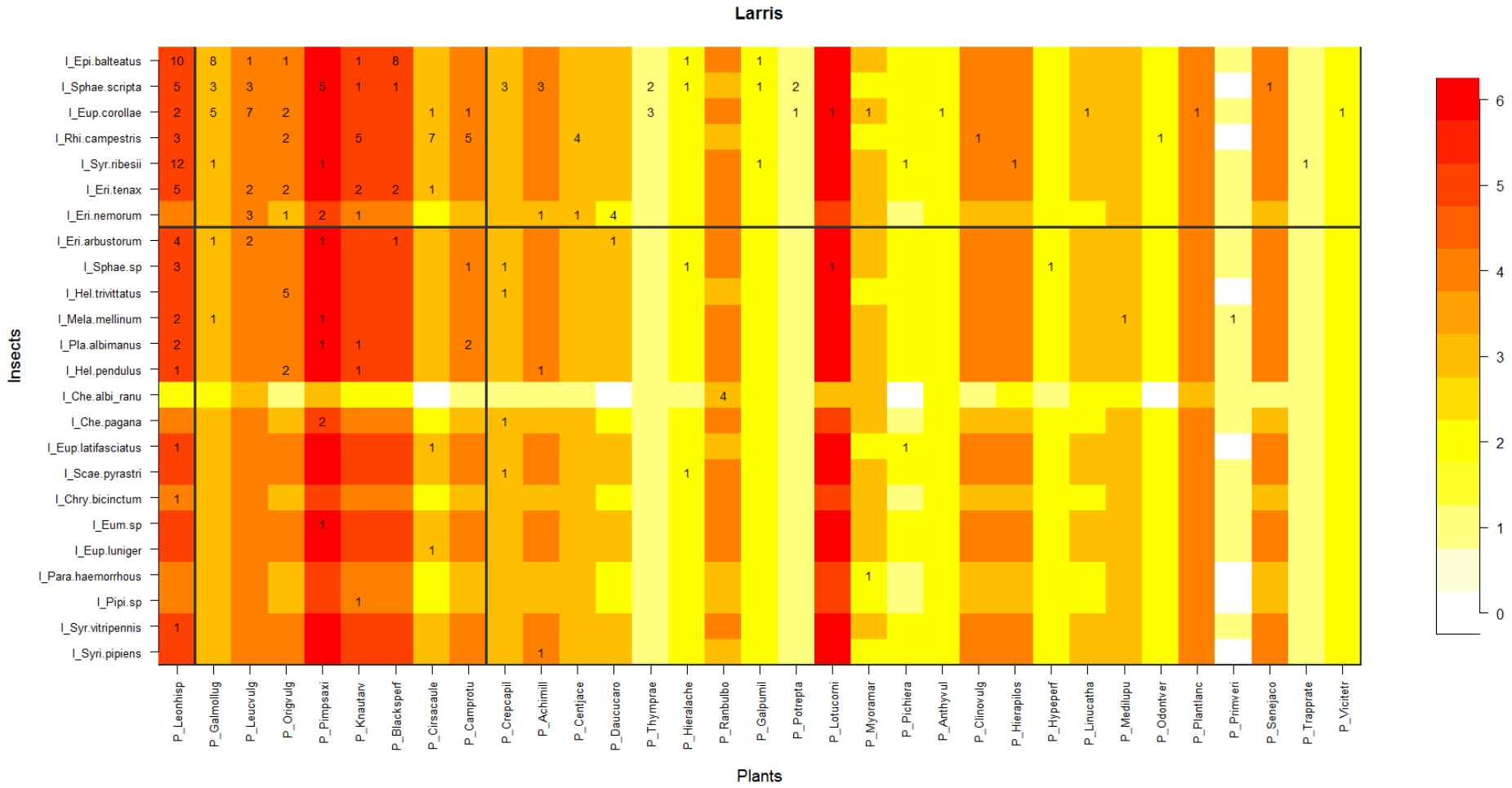

1502

1503 Figure S4. Block clustering provided by LBM in the site of Larris (LAR, Hauts-de-France), overlaid on a heatmap of species phenology overlap. Insect species
1504 are displayed in rows and plant species in columns, following their degree (number of partners). The blocks of insects and the blocks of plants are separated
1505 by solid black lines. Colours correspond to the number of months that are shared by each pair of plant and insect species (PO, phenology overlap), with higher
1506 PO corresponding to darker colours. Numbers are the number of visits observed in the field for a given plant-insect pair.

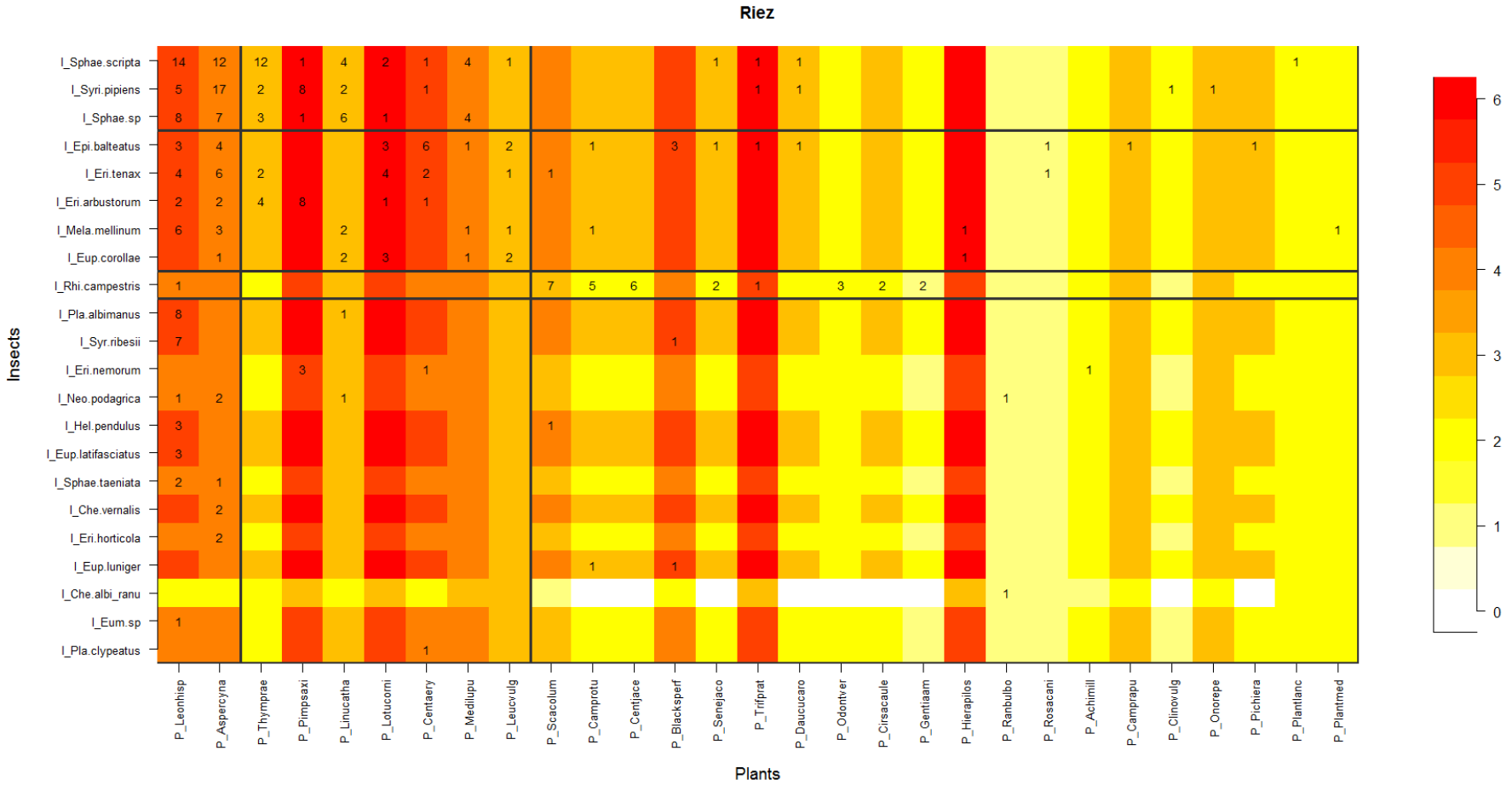

1507

1508 Figure S5. Block clustering provided by LBM in the site of Riez (R, Hauts-de-France), overlaid on a heatmap of species phenology overlap. Insect species are
1509 displayed in rows and plant species in columns, following their degree (number of partners). The blocks of insects and the blocks of plants are separated by
1510 solid black lines. Colours correspond to the number of months that are shared by each pair of plant and insect species (PO, phenology overlap), with higher
1511 PO corresponding to darker colours. Numbers are the number of visits observed in the field for a given plant-insect pair.

Table S1. Table of transformed plant abundances. The first column shows the Braun-Blanquet coefficients of, the second column, their percentages, and the third column, the transformed abundances used as the plant abundances in the model.

Coefficient Braun-Blanquet	Abundance percentage interval	Abundance percentage
i	1 individual	0.1%
+	< 1 %	0.5%
1	1-10 %	5%
2	10-25 %	15%
3	25-50 %	35%
4	50-75 %	65%
5	75-100 %	85%

Table S2. Table of model accuracy. The upper part of the table shows the results of the self-validation: in the region Occitanie the self-validation was tested for the site Bois de Fontaret (BF ~ BF) and the site of Fourches (F ~ F); in the region Normandie for the site of Château Gaillard (CG ~ CG) and the sites of Falaises (FAL ~ FAL) ; and in the region Hauts-de-France for the site of Larris (LAR ~ LAR) and for the site of Riez (R ~ R). The lower part of the table shows the results of the cross-validation only between each site of the same region: in the region Occitanie between Bois de Fontaret et Fourches (BF ~ F and vice versa F ~ BF); in the region Normandie between the site of Château Gaillard and Falaises (CG ~ FAL and vice versa FAL ~ CG); and in the region Hauts-de-France between the site of Larris and Riez (LAR ~ R and vice versa R ~ LAR).

Model type	Region	Sites	Threshold	AUC	Omission rate	Sensitivity	Specificity	Prop correct	Kappa
Self-validation	Occitanie	BF ~ BF	0.15	0.78	0.20	0.80	0.75	0.75	0.22
	Occitanie	F ~ F	0.16	0.78	0.19	0.81	0.74	0.75	0.25
	Normandie	CG ~ CG	0.44	0.75	0.29	0.71	0.79	0.78	0.34
	Normandie	FAL ~ FAL	0.37	0.76	0.16	0.84	0.67	0.69	0.27
	Hauts-de-France	LAR ~ LAR	0.29	0.75	0.16	0.84	0.66	0.69	0.27
	Hauts-de-France	R ~ R	0.27	0.81	0.23	0.77	0.86	0.84	0.53
Cross-validation	Occitanie	BF ~ F	0.15	0.73	0.14	0.86	0.59	0.63	0.20
	Occitanie	F ~ BF	0.16	0.67	0.30	0.70	0.64	0.65	0.17
	Normandie	CG ~ FAL	0.44	0.62	0.45	0.55	0.70	0.67	0.21
	Normandie	FAL ~ CG	0.37	0.68	0.24	0.76	0.60	0.63	0.25
	Hauts-de-France	LAR ~ R	0.29	0.63	0.35	0.65	0.61	0.61	0.17
	Hauts-de-France	R ~ LAR	0.27	0.65	0.42	0.58	0.72	0.69	0.22